Modeling the Neolithic Transition in Europe

Archaeobotanical Aspect of the Expansion of Neolithic Population in Europe

A thesis

submitted in partial fulfilment

of the requirements for the degree

of

Master of Science

in

Statistics

at

The University of Waikato

by

Laeeq Ahmad

THE UNIVERSITY OF
WAIKATO
Te Whare Wānanga o Waikato

2013

Abstract

Whether or not the spread of agriculture in Europe was accompanied by movements of people is a long-standing question in archaeology and anthropology, which has been frequently addressed with the help of population genetic data.

The development and spread of agriculture across Europe is one of the most important events in human history. Studies have addressed questions regarding this Neolithic expansion from three perspectives – the flow of people, the flow of genes, and the flow of culture. Conclusions from these disparate approaches can be contradictory.

The goal of this project is to investigate the movement of the Neolithic people across Europe with respect to Archaeobotany.

Archaeological evidence, radiocarbon dates and genetic markers are consistent with the spread of farming from a source in the Near East.

Data has been collected comprising pollen counts at layers within cores of sediment. Spatial coordinates are associated with each core, and the layers are separated according to a chronology. Identification of a strong and enduring signal of cereal pollen should indicate the arrival of Neolithic migrants to the area, bringing with them the practice of agriculture.

I will be using a diffusion model developed by Davison et al (2006). This model takes a set of parameters and simulates the spread of a population from an original starting point, taking account of factors such as topography and geography. This model might help in the evaluation of results of the observed cereal pollen data from this study, by suggesting whether those results are sensible with respect to the underlying theory of population movement inherent in the diffusion model.

Acknowledgements

I would like to express my deep felt gratitude to my supervisor Dr. Steven Miller for the immense support and excellent advice he has rendered towards my study. You have been extremely supportive and ready to help me whenever I needed help with my thesis. Your kind words of encouragement, reassurance and thorough proofreading kept me going when I had my moments of doubt. I will be forever grateful for all the time and energy you have put into guiding me through this journey, and for always being so efficient, supportive and inspiring.

Your valuable and constructive suggestions during the planning and development of my theses, your help in writing programs in R and your willingness to give your time generously has been highly appreciated. I would not have been able to complete the study without your help and advice.

I would like to thank the University of Waikato and the Faculty of Computing and Mathematical Sciences for their generosity towards granting me an extension. This has given me the opportunity to complete my thesis.

Finally, I would like to express my love and gratitude to my family and friends, especially my wife Durdana and my little daughter Fareeha for supporting me in my endeavour to complete my theses.

"*When we become fully aware that our success is due*

in large measure to the loyalty, helpfulness,

and encouragement we have received from others,

our desire grows to pass on similar gifts.

Gratitude spurs us on to prove ourselves worthy

of what others have done for us.

The spirit of gratitude is a powerful energizer."

by Wilfred A. Peterson

Table of Contents

Chapter 4

Chapter 5

Appendix A

Appendix B

Appendix C

List of Figures

Chapter 1

Introduction

The Neolithic period refers to the interval in the development of human technology that corresponds with the end of the so called “Stone Age", before the widespread adoption of metal tools. The period of human history in Europe covered by the Neolithic period extends from approximately 7000 years to 3500 years BCE (Before the Common Era). The introgression of the Neolithic culture into Europe is thought to have come from its birthplace in the Middle East, originating approximately 9500 years BCE as suggested by Childe (1925).

Neolithic culture is characterized by the development of agriculture. The domestication of wild plants and animals, in particular cereals and later cattle, allowed Neolithic people to abandon the hunter-gatherer lifestyle. Relying on domesticated stock and crops allowed permanent settlements to be developed, and land could support higher population densities.

I will be modeling the expansion of Neolithic people throughout Europe and comparing it with the spread of radiocarbon dated fossils of cereal pollens found in the lake sediment cores throughout Europe and Russia. This process produced several forms of evidence. Stone tools and characteristic pottery are two examples of archaeological evidence for the Neolithic transition. Such artifacts are rare however,

they may not be readily radio-carbon dateable, and pottery in particular may be evidence of a cultural diffusion, without necessarily providing evidence of a movement of people.

1.1 Population Diffusion

Here, I am interested in the movement of Neolithic people across the European continent over a period of several thousand years. At such scales of space and time, modelling individual movement events is essentially intractable. Instead, the theory of particle diffusion can be used to approximate the spread of migrant populations over the time period specified.

A general definition of diffusion given by Okubo (1980) is a regular dispersion movement of groups of particles arising from the irregular motion of the particles themselves. In the case of this study, the particles refer to individual or small groups of migrants. Irregular motion can be taken as a Brownian-like movement of groups across topography. The wave-of-advance model of population movement, suggested by Ammerman and Cavalli-Sforza (1971), advocates such irregular movement. As such, using a diffusion approach necessarily assumes the wave-of-advance model for population movement. Critics of such a model would advocate a more individual specific model of population movement, which in all probability produces more

accurate results, but at the expense of computational efficiency due to the increased complexity. But studies have also shown that diffusion can be the consequence of random walks of individuals over homogeneous landscape, so it should be a good approximation.

Part of the efficiency of diffusion models results from their definition as partial-differential equations over space and time. This allows for the change in concentration of the particles (or the change in population density, for our purposes) to be expressed as a relative change per unit time. Not only does this specification mean that non-standard diffusion scenarios can be handled, but it is relatively trivial to alter parameters across space and time.

Human populations not only **move**, but also **grow**. Introducing a growth (or similarly, death) term to the equation results in what is commonly referred to as a reaction-diffusion model. I use a logistic growth term to model the increase in population density, as is standard. In a realistic scenario there will be both births and deaths within any population, and some populations will experience net population decline and die out. Logistic growth does not allow populations to decrease, but from the macro perspective, loss of individuals frees up resources for new individuals, and the disappearance of small groups will see new groups fill the void relatively quickly. Thus while logistic growth is not appropriate at the individual scale, it is a good approximation at the population level scale we are investigating.

An important consideration is the heterogeneous conditions that affect population spread over a spatial scale. Terrain is a major factor affecting the movement of people. I have incorporated spatially-heterogeneous diffusivity so that movement is hampered at higher altitudes, and at points in water the further they lie from land. At altitude, crops do not grow as easily or yield as much, so they are unable to support such large population densities. The random movement associated with the wave-of-advance model has been described as migration without migrants. This is because there is no need to assume that people purposefully set out to migrate to a new place, but rather, population spread is by a gradual process of each generation moving a relatively short distance from their birthplace to find fresh land to make their own. This type of movement would be immediately retarded at points where crops do not flourish, even if the land is relatively easily traversable by humans. No subsistence is possible in the sea, but crude maritime capability is assumed, allowing the colonization of islands such as Crete and the British Isles. The further a point at sea is from land however, the harder it is for the wave front of a population to advance. Additionally, diffusivity is assumed to decrease at more northerly latitudes, to reflect the lower temperatures and harsher growing conditions.

Finally, consideration must be made of the speculated faster rate of movement along coastlines than through inland areas, as indicated by Davison, Dolukhanov, Sarson and Shukurov (2006). This indicates the possibility that water craft were used to

transport migrants and their animals along coastlines, significantly faster than would have been achieved by foot. The technical term for the preference for movement in certain directions, or directions in which movement can proceed at a faster speed is advection. Here in this study I will model the population diffusion both with and without advection. I will be using faster rate of spread for Mediterranean coastline and Rhine Danube Valley. There is the option for including further water courses which might have aided in the spread of Neolithic migrants into other areas of Europe.

1.2 The Neolithic Expansion

Childe (1925) argued that agriculture, along with number of other innovations, had moved to Europe from its place of origin in the Near East. It is believed that staple crops and herd animals of European Neolithic – wheat and barley, pulses and flax, along with cattle, pigs, sheep, goats – were originally domesticated in the Near East shortly after 10,000 BCE as described by Price (2000). This population in the Near East, around Jericho, in Israel, represents the movement of farmers into Europe as suggested by Zvelebil (1996).

An alternative approach attaches more importance to culture transmission that believes in the adoption of culture traits not necessarily associated with massive long

range travel of individuals as suggested by Whittle (1996). Despite their fundamental difference, both processes represent gradual spread driven by individual random events, either human migration or cultural exchange. Therefore both processes can be modelled with almost the same mathematical equations involving diffusion operator with different parameters.

The simplest model of this type was suggested by Ammerman and Cavalli-Sforza (1973), who choose parameter values for demic expansion. This model neglected any heterogeneity of the environment and only suggested a mild latitudinal gradient in the rate of spread. Even coastlines were neglected in the approximation. Nevertheless, the model was remarkably successful in explaining the constant rate of spread of incipient farming over the vast area of the Near East to Western Europe.

1.2 Archaeological Evidence

Since Vavilov's (1926) pioneering works on the centres of origin of cultivated plants, western Asia and, specifically, the Near East have been considered as the homeland of Europe's agriculture. The earliest indications of agriculture, in the form of cultivation of cereals and pulses, and rearing of animals, come from the Zagros foothills. Their age, 12,200- 7200 BCE as suggested by Bar-Yosef and Belfer-Cohen

(1992), corresponds to the cool, dry climatic period followed by a rapid increase in rainfall at the beginning of the Holocene(10,150-9200 BCE).

During the early stages of agricultural development, the rapid increase in the number of sites is noticeable in both the foothills and the surrounding plains, accompanied by the appearance of large settlements with complicated masonry structures and fortifications (e.g., Jericho). At a later stage, the core area of early agricultural settlements shifts to the north, to the eastern highlands and inner depressions of Asia Minor.

The earliest sites with developed agricultural economies in Europe, dated 6400-6000 BCE, are found in the intermontane depressions of Greece (Thessaly, Beotia and Peloponnese) as mentioned by Perles (2001). Genetic features of the cultigens and the general character of the material culture leave no doubt as to their Near-Eastern origin described by Ozdogan (1997). Significantly, the early Neolithic sites in the Marmara Sea basin are of a more recent age (6100-5600 BCE), being culturally distinct from the Early Neolithic in Greece. This implies that the Neolithic communities could penetrate the Balkan Peninsula from Western Asia by means of navigation. The spread of early agricultural communities further east into the East European Plains, is evinced by Cucuteni – Tripolye sites (Romania, Moldova and Ukraine) of age 5700-4400 BCE as mentioned by Chernykh and Orlovskaya (2004).

All the aforementioned cultural entities bear cultural affiliations with the early agricultural communities of Western Asia, implying that the spread stemmed from

that area. Recent research also identifies a different pattern of the Neolithisation in Europe, less obviously related to the Near East. Numerous pottery-bearing sites have been found along the Mediterranean coastal areas of France and Spain, as well as in the Atlantic coastal regions of France and Portugal. These sites, referred to as Epi-Cardial and Roucadour, show an early age of 7350-6500 and 6400-5500 BCE respectively as suggested by Roussault-Laroque (1990).

There also exists convincing evidence of early pottery making on the East European Plain related to the ages as early as 6910BCE to 5420 BCE mentioned by Dolukhanov, Shukurov et al (2005). This evidence reveals a Neolithic stratum which apparently pre-dated the Near-Eastern wave of advance and later interacted with it.

1.4 Demic Expansion

Since Childe (1925), mass migration from Western Asia or Near East was deemed as the most viable mechanism of Neolithic expansion into Europe. More recent studies done by Price, Bentley, Luning, Gronenborn, Wahl (2001) and Whittle (1996) attach greater significance to the indigenous adoption of agriculture, described as culture transmission, driven by contacts between invading farmers and local foragers. It is clear, however, that some human migration occurred at each stage of Neolithisation. According to Harris (1996) and Troy et al. (2001), the genetic evidence convincingly proves the Near Eastern origins of the major domestic animals and plants such as sheep, goat, cattle, pig and barley wheat and pulses respectively. Human DNA also

demonstrates that at least 10 to 15 percent of the existing genetic lineages were introduced into Europe in the course of Neolithisation from the Near East as mentioned by Richards et al. (1996). Also, early Neolithic archaeological assemblages in South Eastern and Central Europe in most cases have little or no common elements with the preceding Mesolithic cultures, implying the influx of new populations.

On the other hand, there is sufficient evidence that groups of hunter-gatherers were variably involved in the process of Neolithisation. This is suggested by the occurrence of Mesolithic-type lithic tools in several early agricultural assemblages and presence of cereal pollen on some sites well before the Neolithic period. Strontium-isotope analysis of skeletal remains at several sites in the Rhine Valley strongly suggests intermarriages between farmers and hunter-gatherers as described by Gronenborn (2003). Significantly, both direct migration and cultural transmission resulted in a significant population growth.

Discussing the Neolithic expansion, one should consider several important environmental constraints. All early farming sites were located in areas with fertile and easily arable soils, and in close proximity to water reservoirs (lakes or rivers). Mixed broad-leafed forests with natural clearings were evidently favoured by early farmers. The natural habitats of early agricultural settlements enjoyed a considerable amount of rainfall and sufficiently high temperature during the vegetation period, which facilitated a satisfactory yield. Significantly, the periods of major agricultural

advances coincided with the periods of increased temperature and rainfall (the Holocene climatic optima).

It is thus clear that farmers' migration into Europe did not occur in a uniform way; indeed spatial variations in the propagation speed of the land farmers have been noted as described by Ammerman, and Cavalli-Sforza (1971), Clark (1965) and Fort and Mendez (1999). This is not surprising when the heterogeneity of the spatial domain, Europe, is considered.

1.5 Cereal Pollen

Pollen in the lake sediment reflects the historical vegetation as described by Haslett et al (2006).

The European Pollen Database (EPD) contains records of 102901 entries of pollen whether cereal or wild, for 891 separate sediment cores across Europe and Russia with 2468 pollen taxa describing 381 genera. (http://www.europeanpollendatabase.net/data/). 627 of these cores detect pollen associated with cereal at least once at some depth in any sample. There are 872 core sites which show no evidence of cereal in some of the samples at different depths. There are clearly some core sites which show cereal pollen at some depths but none on the other depths. It will be necessary to determine whether this is because the

analysts were not recording the presence of cereal pollen, or whether there was truly no cereal pollen present in the cores. These sites are shown in the Figure 1.1.

As there were 1108 workers involved in the process of collecting and analysing the data and many of them might have different criteria for doing their work so it will be wise in the future to check the authenticity and reliability of the data and see if every one of the analyst was recording the pollen data consistently.

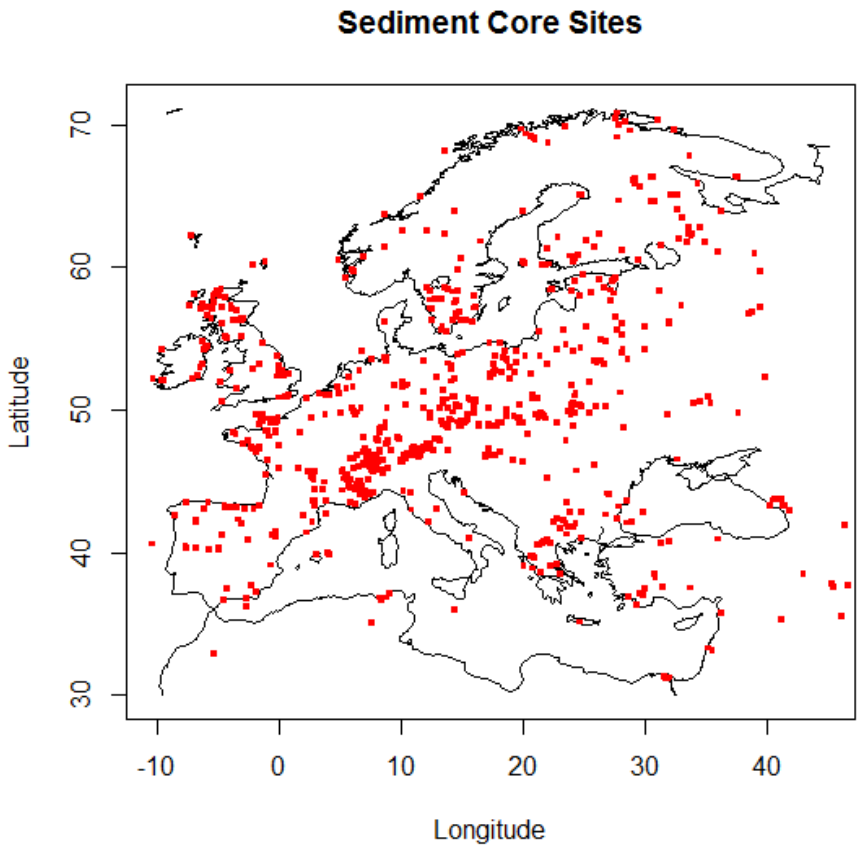

Figure 5.1 Plot of Sediment Core Sites in Europe and Near East.

Additionally, there is uncertainty in the pollen counts, for example due to sampling uncertainty arising from the sampling site, and the volume of the slice, as the thickness and the width of the slices vary from 0.5 to 25 and 2 to 108 cm respectively. Further variation may be possible due to observers' uncertainty such as in the correct identification of cereal pollen.

The signal regarding the advance of Neolithic farmers bringing their cereal crops is subject to a large degree of noise. Stochastic effects from wild grasses, and the unintentional transitory dispersal of cereal by wind or birds will affect the detectability of the signal, as will the low-level and short-term cultivation of some cereals (particularly wild cereals) by earlier Mesolithic cultures as we have found some data associated with cereal well before 10 000BCE as shown in Figure 1.2.

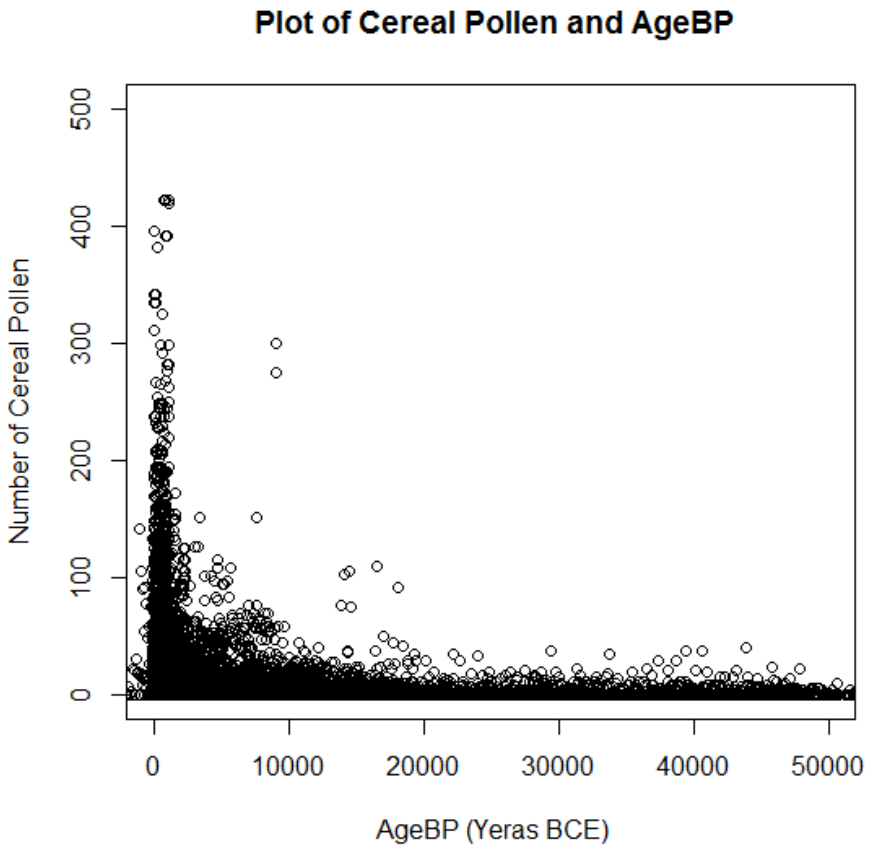

Figure 2.2 Plot of Cereal Pollen and AgeBP in Europe and Near East from 0BCE to 50000BCE.

Figure 1.3 is another plot of the cereal pollen that had radiocarbon ages of less than 10,000 years BCE or before the Neolithic era. It is clear from Figure 1.3 that there was cereal pollen in Europe well before the Neolithic or probably before even the Mesolithic era. Although there are occasional spikes in the plot which can be due to random error associated with the data or some human error during the collection of the data, the presence of cereal pollen cannot be ruled out because of these errors.

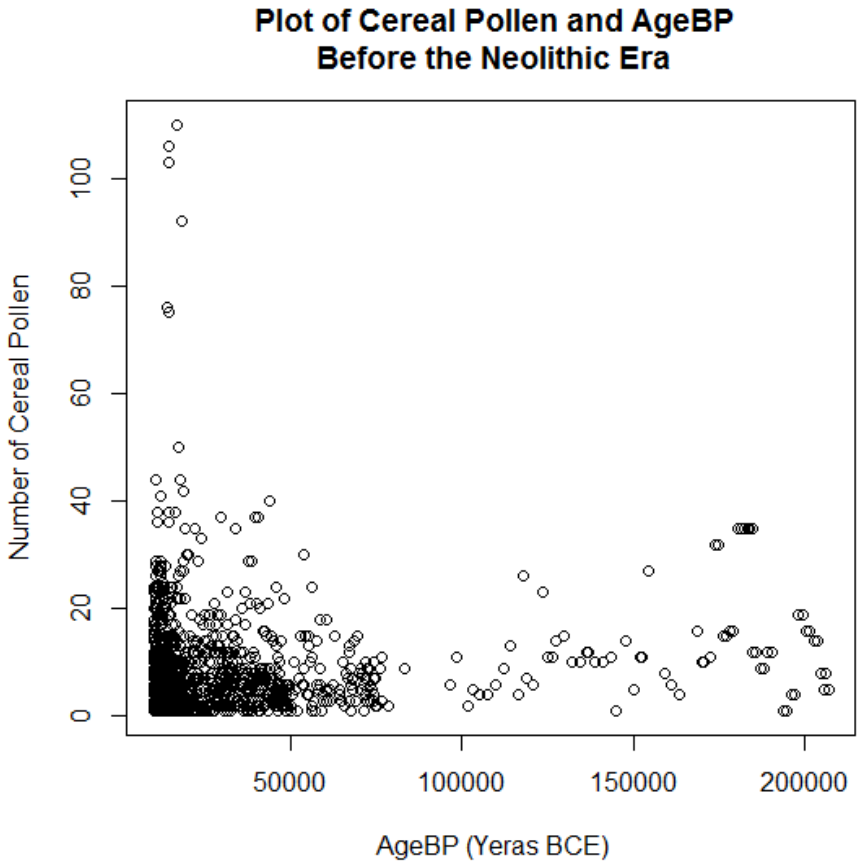

Figure 1.3 Plot of Cereal Pollen in Europe and Near East before the Neolithic era.

For this project, I am focusing on cereal pollen deposited on lakebeds during the Neolithic expansion, and now available through lakebed core samples. The organic material in sediment layers which contain pollen.

Radiocarbon dating, or simply carbon dating, is a technique to estimate the age of organic materials that was first presented by a team of scientists lead by Libby (1960). This was later well outlined by Taylor (1987).

Chapter 2

Collection and Exploration of the Data

To model the spread of the Neolithic people through Europe, we have access to data involving fossil cereal pollen from the European Pollen Database (EPD) which is a freely available database of pollen frequencies, past and present, in the larger European area.

These data are indicators of the spatial-temporal demographic flow of people over the landscape. We therefore develop a demographic model for this population flow, and use the observed data to produce posterior support for key parameters governing this spatial-temporal process.

2.1 The Pollen Data Collection

As the Neolithic people moved through Europe, they will have established settlements that relied on agriculture involving cereals. As these settlements became established, the pollen from the domesticated cereal crops would find its way into the

sediment of nearby lakes. As new layers of sediment were laid down, the pollen became fossilized. Cores of lake sediment have been recovered from many sites across Europe. These cores have been divided into slices, and counts of pollen in each slice have been recorded and classified by species. In some instances, cereal pollen is aggregated along with pollen from other closely related grass species. However, in many cases, cereal pollen counts are available from these mud cores, although it is not always indicated whether the cereal is from wild or domesticated species.

A selection of slices from the mud cores are combed for organic material that is suitable for radio-carbon dating.

We assume, there are three processes that lead to the deposition of cereal pollen in lake sediment. The most important, and the process I am interested in, is the Neolithic transition. This process sees an increase in the amount of cereal pollen found in the sediment proportional to the size of the Neolithic population in the area over time. Once a Neolithic population becomes established in an area, we might expect the level of cereal pollen remains constant from that point forward in time. There will also be occasional spikes of pollen presence. That is, instances where there is an indication of pollen presence of a periodic nature. This could be due to factors such as short-term flourishing of wild cereal in the area, by chance or through cultivation by a transitory Mesolithic population. The third process is random noise, which incorporates events such as long-distance wind dispersal of cereal pollen, or dispersal by migratory birds, as well as the error associated with the identification and enumeration of cereal pollen in sediment slices.

2.2 Quality of Data

As the data have some extreme values in the number of pollen associated with cereal and there are some other level of uncertainty so we have to check the quality of the data. At this stage we are unable to contact every person involve in the collection and processing of this data set to verify the suitability of this data set for our purpose but it can be done in future if necessary.

There is a core site Dunum (Hilliges Moor, Germany), where, there is highest number of cereal pollen (908, 908, 1208, 1208, 1384, 1384, 2512, and 2512). All other sites have fewer than 500 of cereal pollen so I have decided to ignore this core site in our modelling as well. Furthermore there are a lots of zero cereal pollen in the data set, roughly two third of the data set have zero cereal pollen. There is no point including those values in the data set as it will make the plots look a bit messy so I will also ignore these zero entries in the model. Also one, two, three and four cereal pollens in the data set might have been the result of some noise in the process of collecting and recording the data, so for the simplicity, I will also leave those entries as well.

The plot with five or more pollen in any sample at any core site ignoring the only one site Dunum (Hilliges Moor, Germany), and with the radiocarbon dating up to 10,000 BCE is as under:

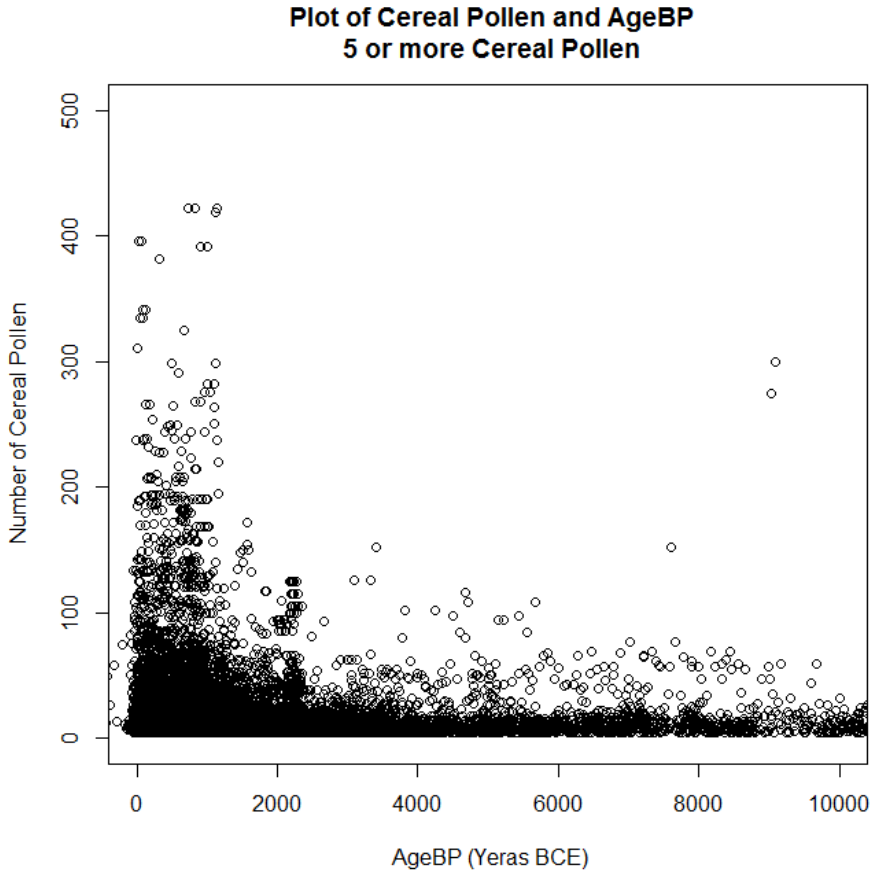

Figure 6.1 Plot of Cereal Pollen and AgeBP in Europe and Near East with 5 or more Pollen at a Sediment Site.

It is clear from the Figure 2.1 that there is lot on noise in the data set and some sites have some odd values as well. I will check it with respect to site locations if there is any pattern in any location.

2.3 Good Location Examples

Here in the following three figures, it is clear that the data set look in a bit better form. The Figure 2.2 shows the plot of cereal pollen on the sediment core site "Charco da Candieira", shown by red dot, which is in Portugal. It is clear that the cereal pollen found there was started at 4605 BCE and they gradually increased in numbers with the passage of time. The black dot represents the supposed starting point (Jericho) of the population diffusion of the Neolithic expansion in Europe. That means the population may have been started there at around the same time. Similarly Figure 2.3 represents the data at sediment core site "Alsópáhok", which is in Hungary as shown by red dot on the plot. It is clear from the figure that the cereal pollen found there was started at 3205 BCE which means that it might be the time when Neolithic people started their settlements in that area. Figure 2.4 shows the data of cereal pollens from the sediment core site "Ageröds Mosse", which is in Sweden as shown by red dot. It shows that pollen arrives there at 1640 BCE as with the Neolithic population. There is a possibility that these data set are subject to some random noise and other errors during the collection and recording of the data.

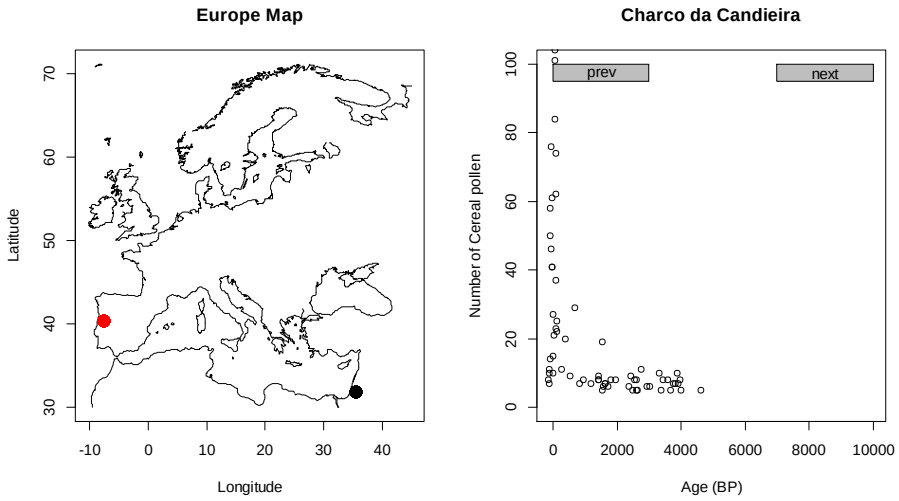

Figure 2.2 Plot of Sediment Core Site "Charco da Candieira" and "Jericho" on the map of Europe and Near East with number of Cereal Pollen and AgeBP at the same Location.

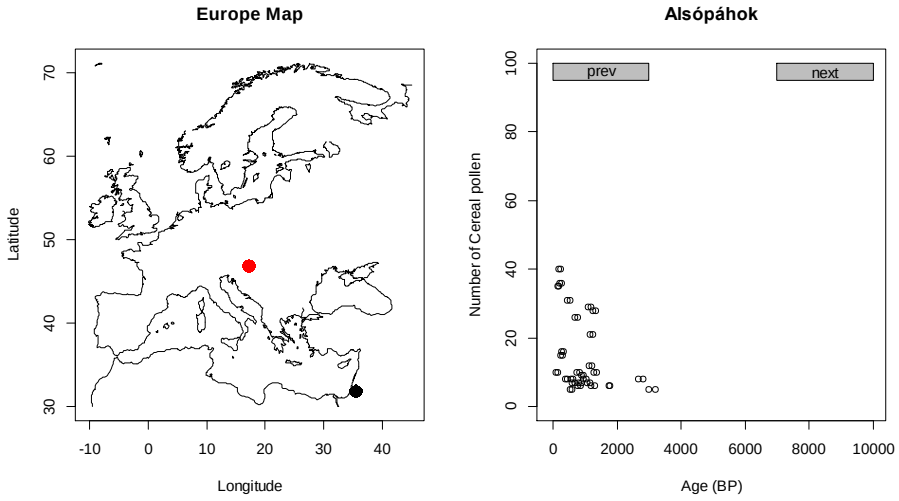

Figure 2.3 Plot of Sediment Core Site "Alsópáhok" and "Jericho" on the map of Europe and Near East with number of Cereal Pollen and AgeBP at the same Location.

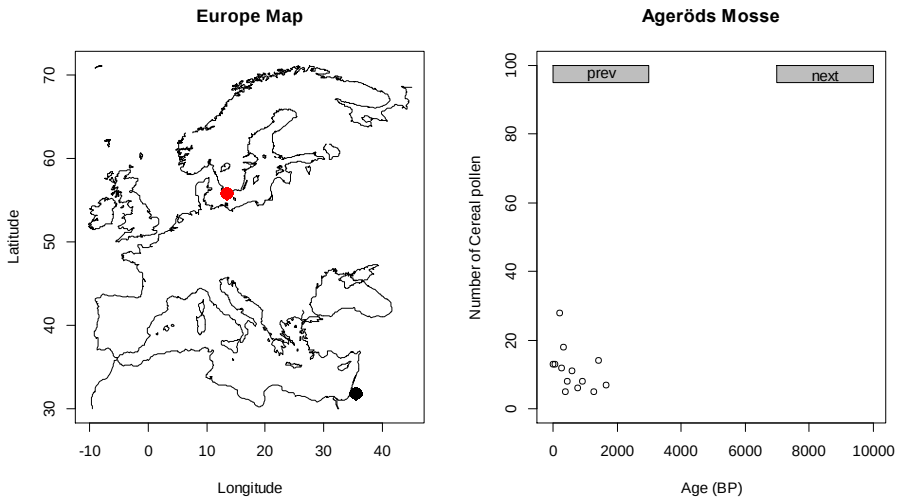

Figure 2.4 Plot of Sediment Core Site "Ageröds Mosse" and "Jericho" on the map of Europe and Near East with number of Cereal Pollen and AgeBP at the same Location.

2.4 Bad Locations Example

As for good examples of the data set, there are some bad examples as well where data does not look too good. The Figure 2.5 here is of the sediment core site "Antas", shown by red dot on the plot, which is situated at the south-western coast of Spain, It shows some cereal pollen there as early 8744 BCE, but there is no data showing in the data set after 6188 BCE. According to assumed starting point "Jericho", it is not possible for Neolithic people to reach as far as Spain at that point of time so these pollens might have been from some of the Mesolithic people who might have been in

that area for some time and was growing cereal crops. The unavailability of more data could have different reasons which may include but not limited to the not counting of the cereal pollen for that particular sediment core site. Similarly Figure 2.6 shows second sediment site “Akgöl Adabag”, which is in Turkey and represented by red dot on the plot, shows only one entry of cereal pollen at 9746 BCE and Figure 2.7 shows the third sediment core site “Aghia Galini”, which is in Crete, Greece, and represented by red dot shows only three records of cereal pollen in the data set from 8257 BCE to 7455BCE. There could be lot of reasons why there is no more data available for these locations. The one possibility is that the person collecting the data at that time may not be counting the cereal pollens or they might have misclassified those pollens and so on. It will be a good idea in if the data can be verified at a future stage.

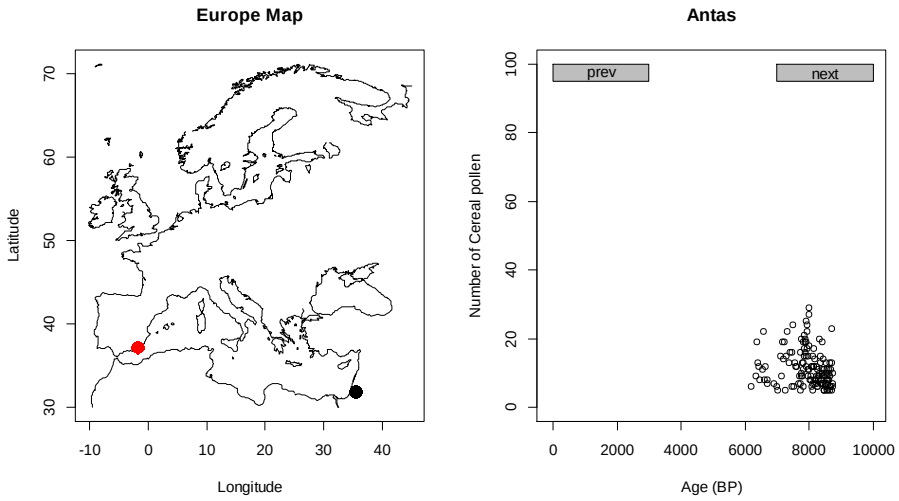

Figure 2.5 Plot of Sediment Core Site "Antas" and "Jericho" on the map of Europe and Near East with number of Cereal Pollen and AgeBP at the same Location.

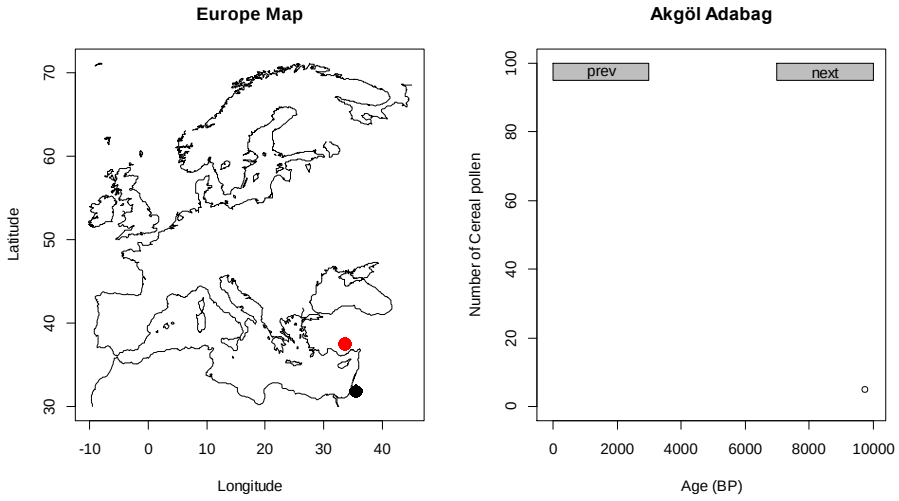

Figure 2.6 Plot of Sediment Core Site "Akgöl Adabag" and "Jericho" on the map of Europe and Near East with number of Cereal Pollen and AgeBP at the same Location.

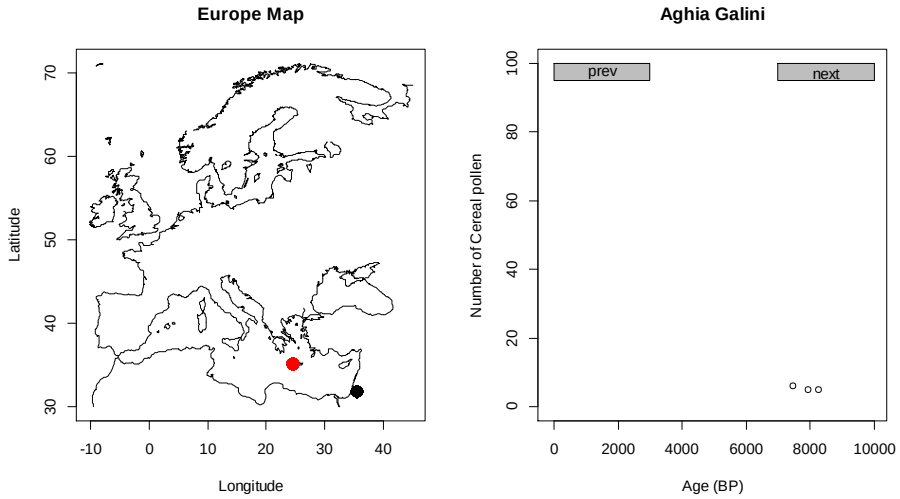

Figure 2.7 Plot of Sediment Core Site "Aghia Galini" and "Jericho" on the map of Europe and Near East with number of Cereal Pollen and AgeBP at the same Location.

The above examples of good and bad data set are only a few which was mentioned here. It will be a good idea to clean the data if possible before any further processing and also check the reliability of the data and possible reasons for missing data. Unfortunately, due to time restriction, it is not possible to do that at this stage but it will be worthwhile to do so in future.

Chapter 3

Methods and Modelling of the Data

3.1 The Demographic Model

Here, I will model the underlying demographic flow at the population level, by using the differential equation described by Davison et al. (2006) and also used by Davison, Dolukhanov, Sarson, Shukurov and Zaitseva (2009).

$$\frac{\partial D}{\partial t} + (V \cdot \nabla)D = \gamma D\left(1 - \frac{D}{K}\right) + \nabla \cdot (\upsilon \nabla D)$$

This equation describes the evolution of the population density at any position, D (θ,ϕ,t). Here the equation is applied at the spherical surface of the earth, whose radius is approximately 6356.7523 km (This is polar radius of the earth. The equatorial radius of the earth is 6,378.1370 kilometers. One can use the either one). θ and ϕ are latitude and longitude respectively (θ = 0 on North Pole). I have noted in this connection that deviations from planar geometry become quite pronounced on the global length scales involved, and front propagation rates inferred from planar models can be significantly in error.

The significance of the various terms in the above equation is as follows:

D	is the population density at latitude θ, longitude ϕ and time t.
t	is time.
V	is the advection velocity across latitude and longitude.
γ	is the population growth rate coefficient or intrinsic growth rate measured in inverse years.
K	is the population carrying capacity at a location measured in person/km^2.
υ	is the diffusion coefficient or diffusivity.
$\frac{\partial D}{\partial t}$	is the net rate of change of the population density with time at a given position.
$\gamma D\left(1-\frac{D}{K}\right)$	is the basic logistic growth term.
$\nabla.(\upsilon \nabla D)$	is the diffusion resulting from random migration events quantified by diffusivity υ.

Both "γ" and "K" may vary in space to model the variation in the habitat's ability to support the population. Similarly, "υ" and "V" can vary in space to reflect heterogeneity in the rate and ease of movement.

This equation can be described as a reaction-advection-diffusion as suggested by Hundsdorfer and Verwer (2003).

Reaction refers to demographic processes such as birth and death, as well as interaction between particles during the diffusion. We model population growth as a logistic function with growth rate, with upper carrying capacity "K". Both "γ" and "K" are modeled as functions of altitude and latitude, so that populations grow more slowly and land can support lower population densities at higher altitudes, and towards the northern latitudes. Population growth is not permitted at locations found in the ocean. Reaction can also describe the interaction between particles in the diffusion

Advection refers to preferential movement in particular directions. Because I am modeling migration at the population level, I am assuming that the particles in our system diffuse according to the Fickian heat diffusion model by Fick (1855), leading to an isotropic expansion away from areas of higher population density at rate "υ". In this model, the diffusion rate also decreases with decrease in latitude and increasing altitude, representing the greater difficulty of migration in colder conditions. The rate of diffusion decreases exponentially over water as the distance to the nearest land increases. Previous studies have noted how there is evidence that appears to suggest Neolithic migrants were able to move faster along coastlines and major inland waterways, such as the Rhine- Danube river system, possibly through the use of rafts to transport people, livestock and possessions. To allow for this possibility, an advection velocity "V" is incorporated, that allows for preferential movement over a vector field following coastlines and the Rhine-Danube system.

The diffusion model is implemented by overlaying the landscape with a grid, then using the finite difference approximations described by Euler's method to reconstruct the diffusion over space and time. The accuracy of this approximation to the diffusion over continuous space and time is improved as the distances between grid points and between times increments decrease.

3.2 Application of the Model

The propagation of land farming throughout Europe has attracted sustained interest in recent years like Ammerman and Biagi (2003). Edmonson (1961) conducted a pioneering study into Neolithic diffusion rates. His empirically relevant hypothesis was that the apparent propagation speed of simple, rational Neolithic traits, such as copper or pottery, was approximately constant; he estimated it to be 1.9 km/year. This estimate applies to a far larger area than Europe. Edmonson also assumed that he was measuring cultural transmission.

On the other hand Ammerman and Cavalli-Sforza (1971) measured the rate of spread of early farming in Europe on the basis of a single trait (cereals) and restricted their study to a far more specific geographical area. They derived the rate of spread to be 1 km/year on average in Europe and this estimate has remained widely accepted since then. They also noted very significant regional variation in the rate of spread due to unfavourable ecological and geographical factors such as high altitude and coastlines etc. Zilhao (2001) also mentioned that the propagation speed should have been

decreased at latitude above 54^{o} N and there should have an increased propagation spread along the Mediterranean coast and the Danube and Rhine valley.

According to the estimates from the above mentioned studies, the speed of propagation of the wave front in these areas are as follow:

1 km/year	on average in Europe,
4-6 km/years	for Danube Rhine valleys,
10 km/years	for Mediterranean coast.

Interpretations of these observations are usually based on the reaction-diffusion equation of population dynamics, the Fisher, Kolmogorov, Petrovskii, Piskunov (FKPP) equation, as mentioned by Fisher (1937) and Kolmogorov, Petrovskii and Piskunov (1937). The constant propagation speed of the population front is a salient feature of solutions to this equation in one dimension described by Murray (1993). However, applications of this approach to the spread of the Neolithic in Europe have hardly advanced beyond simple one-dimensional models in a homogeneous environment.

The results of Ammerman and Cavalli-Sforza (1971 & 1973) have also been confirmed by Gkiasta, Russell, Shennan and Steele (2003), who used a much more comprehensive radiocarbon database. These authors suggested that the regional variations in the spread may be due to variations in the importance of demic versus cultural transmission, with the former leading to a more abrupt transition.

While much work has been carried out into the measurement of the Neolithic dispersal, work on modelling this phenomenon is sparse. Fort and Mendez (1999) discuss the front propagation speed resulting from various generalisations of the FKPP equation, but their results are restricted to one dimension and to homogeneous systems. Currat and Excoffier (2005) has developed a model which takes into account the influence of heterogeneous environments on the spread of farming, and models it more realistically in two dimensions. Steele, Adams and Sluckin (1998) modelled the dispersal of hunter-gatherers into North America using a two-dimensional numerical model where spatial variation in the carrying capacity was allowed for (as suggested by paleovegetation reconstructions). These authors note that the diffusivity (mobility) of people must also be a function of position and time, and suggest that the spread might have followed major river valleys, like, Anderson (1990) , but do not include these effects into their model.

3.3 Model Parameters

Steele et al (1998) with many other authors, suggest the range 0.003-0.03 per year for the intrinsic growth. So, here I will take

$$\gamma = 0.02 \text{ /year}$$

which is consistent with the population doubling in 30 years. Dolukhanov (1979) estimates the carrying capacity for hunter gatherers in a region of temperate forest to

be 7 persons per 100 km^2. Ammerman and Cavalli-Sforza (1984) suggest that the carrying capacity for farmers is a factor of 50 larger, which results

$$K = 3.5 \text{ persons/km}^2$$

Although Europe was not all temperate forest, it is wise to use this constant value as it has been shown by Davison et al (2006) that the model which is used for the front propagation speed is independent of "K", and so this choice does not affect the propagation speed. Taking the speed of propagation of the wave front as one kilometre per year as mentioned by Ammerman and Cavalli-Sforza (1971), results in the υ = 12.5 km^2/year as the background diffusivity as used by Davison et al (2006). But here in this study, various values of υ are used at different locations depending on the different parameters like altitude. The magnitude of the advection velocity is based on the variations in the speed of propagation of the wave front.

Chapter 4

Results and Discussion

4.1 Plotting the Data

The map of Europe and Near East is plotted by using the data of the coordinates of longitude and latitudes available at National Geophysical Data Center. The National Geophysical Data Center (NGDC), located in Boulder, Colorado, is a part of the US Department of Commerce (USDOC), National Oceanic & Atmospheric Administration (NOAA), National Environmental Satellite, Data and Information Service (NESDIS). http://www.ngdc.noaa.gov/mgg/coast/

As the horizontal length of Europe is approximately 3300 miles so here I divided the Europe and Near East into 331×331 grid cells. Each grid cell is one mile in each dimension. Also I have used 331×331 matrices for the values of advection velocity "V", intrinsic growth rate "γ", population carrying capacity "K" and diffusion coefficient "υ". Even though the vertical length of Europe is not 3300 miles but I have decided to use the square matrices as it will give top of the North Africa as well, which is probably a possible corridor for Neolithic transition in Europe.

The data set of cereal pollen from the European Pollen Database has been sorted by using Access and Excel software from Microsoft. R has been used for all the statistical computing and graphics produced in this study.

As the Neolithic period starts from 7000BCE to 9500BCE so I have decided to take 8000BCE as the starting point for the Neolithic Population. Jericho, as mentioned earlier, will be considered as the starting point for the Neolithic expansion into Europe. There is the possibility that more than one advance was made into Europe at the same time, potentially from different directions. But at this stage I have only focused on one starting point.

A diffusion function is created in R (See Appendix B) and used to simulate the possible expansion of the Neolithic population starting from Jericho at 8000BCE and the results were recorded every 1000 years. The results from this simulation are compared with the actual data of cereal pollens from the EPD.

4.2 Goodness of fit

To check if the simulated model is a good fit of the observed data, cereal pollen is coded as a binary variable, either present or absent, across space and time. Here I assume that there is a small time difference between the arrival of the wave front of Neolithic expansion and the deposition of identifiable quantities of cereal pollen in sediment by choosing to designate the presence of cereal pollen at a site only after the

population density at a site exceeds 0.5 persons per square kilometer. To test the robustness of the model to error in identifying the presence of cereal pollen due to random chance, or the influence of factors not associated with the Neolithic expansion, I set a probability β for correctly identifying the presence or absence of pollen at any given site. In this way, at any point of time, there might be (1- β) ×100% of sites to incorrectly code the presence or absence of Neolithic settlers due to the presence or absence of cereal pollen.

4.3 Calculating the Goodness of Fit

The pollen data is recorded as either pollen being present or absent. Because the demographic process is deterministic, it is easy to create a flow of Neolithic people given a set of parameters. Therefore, it can be written as

$$f(x_p|\theta_d) = f\{x_p|x_p^*(\theta_d)\}$$

where $x_p^*(\theta_d)$ is the resulting collection of pollen presence/absences expected, based on the population densities simulated from a set of parameters provided. Then

$$f(x_p|\theta_d) = \beta^{n-\sum_{i=1}^{n}|x_{p;i}-x_{p;i}^*|}(1-\beta)^{\sum_{i=1}^{n}|x_{p;i}-x_{p;i}^*|}$$

where $x_{p;i}$ is the observed presence of pollen at the *i*th space-time coordinate, and $x^*_{p;i}$ is the simulated presence of pollen at the *i*th space-time coordinate, given the demographic parameters θ_d.

Taking the log-likelihood we get

$$\log\left[f\left(x_p\middle|\theta_d\right)\right] = n\log(\beta) + \log\left(\frac{1-\beta}{\beta}\right)\sum_{i=1}^{n}\left|x_{p;i} - x^*_{p;i}\right|$$

The following results are indication of goodness of fit.

4.4 Plots and Results

I have simulated the possible expansion of the Neolithic population by using no advection at first and then I used the advection with a possible faster movement along Mediterranean coastline and Danube Rhine valleys. The consideration was also given to the slow movement at higher altitudes. Here are the resulting plots of the calculations

4.5 Without Advection

At 7000 BCE

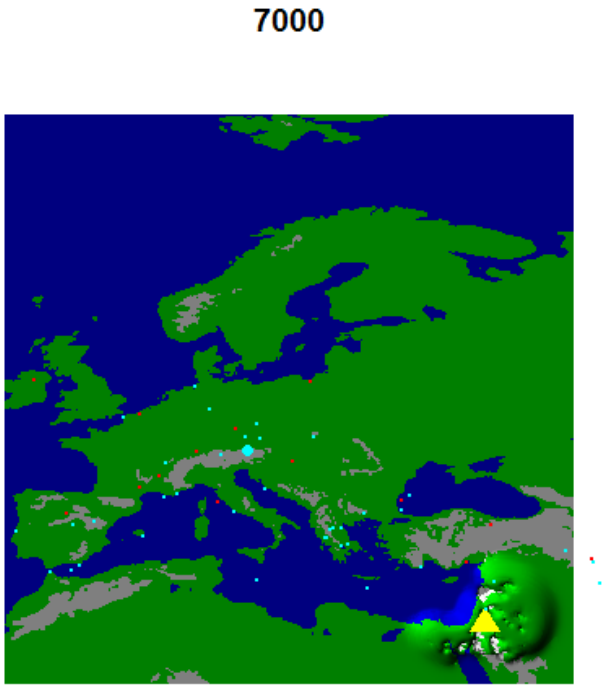

Figure 4.1 Simulation of the Neolithic Population in Europe and Near East at 7000BCE.

The Figure 4.1 show the simulation of the Neolithic population with no advection, at 7000BCE. The starting point is Jericho, which is represented by yellow triangle in the

plot. The sites of cereal pollen are shown by dots. Red dots represents the pollen sites from 10000BCE up to 7000BCE whereas the cyan dots shows the location of cereal pollen at that particular age bracket i.e. from 8000BCE to 7000BCE.

It is clear from the Figure 4.1 that there are not many site locations that matches the simulation. Only 2 site locations out of 53 site locations of cereal pollen are matched whereas simulation is showing 4 possible site locations. There are many site locations that are outside of the simulation, even outside of our Europe map, which is not a good fit at this stage. There could be many reasons to justify this such as the data or the carbon dating process may have some errors or there might be some cereal pollens at some place before the Neolithic era.

At 6000 BCE

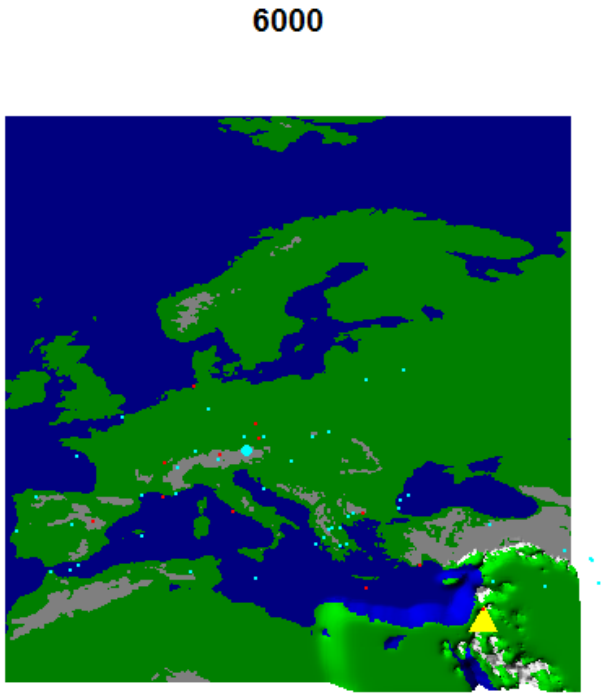

Simulation with Cereal Pollen Sites marked with Red Dots.
Dots in 'Cyan' color represents the Cereal Pollen in that Age Bracket.
'Jericho',The Origin is mentioned with yellow triangel.

Figure 4.2 Simulation of the Neolithic Population in Europe and Near East at 6000BCE.

The Figure 4.2 show the simulation of the Neolithic population with no advection at 6000BCE. The starting point is Jericho, which is represented by yellow triangle in the plot. The sites of cereal pollen are shown by dots. Red dots represents the pollen sites from 10000BCE up to 6000BCE whereas the cyan dots shows the location of cereal pollen at that particular age bracket i.e. from 7000BCE to 6000BCE.

Again, it is clear from the Figure 4.2 that there are not many site locations that matches the simulation. Only 6 site locations out of 122 site locations for cereal pollen are matched this time whereas simulation is showing 10 possible site locations. There are many site locations that are outside of the simulation, even outside of our Europe map, which is not a good fit at this stage. There are probably the same reasons to justify this such as the data or the carbon dating process may have some errors or there might be some cereal pollens at some place before the Neolithic era.

At 5000 BCE

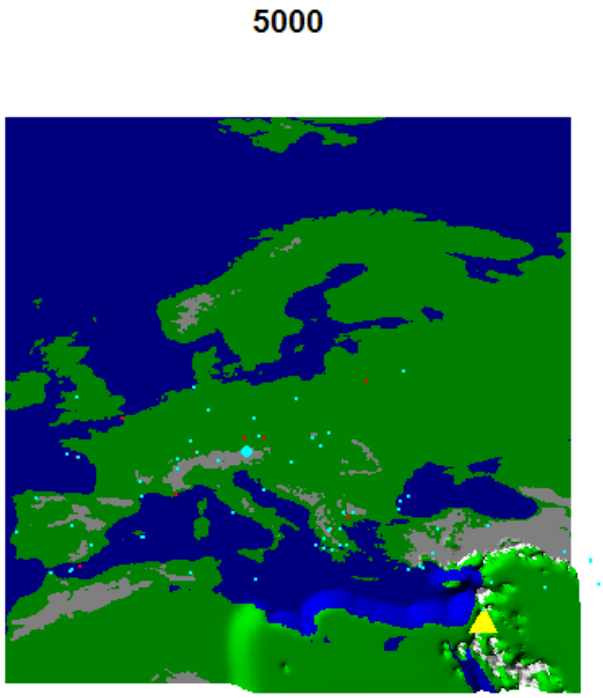

Figure 4.7 Simulation of the Neolithic Population in Europe and Near East at 5000BCE.

The Figure 4.3 show the simulation of the Neolithic population with no advection at 5000BCE. The starting point is Jericho, which is represented by yellow triangle in the plot. The sites of cereal pollen are shown by dots. Red dots represents the pollen sites from 10000BCE up to 5000BCE whereas the cyan dots shows the location of cereal pollen at that particular age bracket i.e. from 6000BCE to 5000BCE.

Again, it is clear from the Figure 4.3 that there are not many site locations that matches the simulation. Only 10 site locations out of 217 site locations of cereal pollen are matched whereas simulation is showing 16 possible site locations. There are many site locations that are outside of the simulation, even outside of our Europe map, which is not a good fit at this stage. There could be the same reasons to justify this such as the data or the carbon dating process may have some errors or there might be some cereal pollens at some place before the Neolithic era.

At 4000 BCE

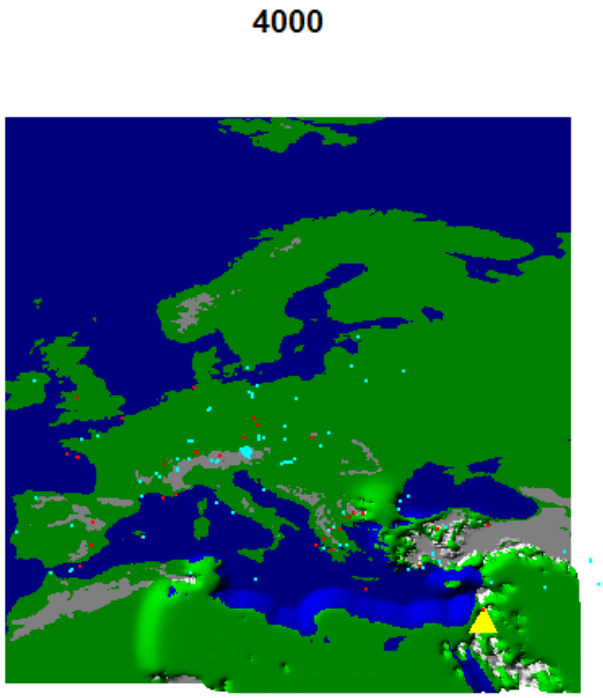

Figure 8.4 Simulation of the Neolithic Population in Europe and Near East at 4000BCE.

The Figure 4.4 show the simulation of the Neolithic population with no advection at 4000BCE. The starting point is Jericho, which is represented by yellow triangle in the plot. The sites of cereal pollen are shown by dots. Red dots represents the pollen sites from 10000BCE up to 4000BCE whereas the cyan dots shows the location of cereal pollen at that particular age bracket i.e. from 5000BCE to 4000BCE.

It is clear from the Figure 4.4 that there are not many site locations that matches the simulation. Still only 20 site locations out of 346 site locations of cereal pollen are matched whereas simulation is showing 33 possible site locations. There are many site locations that are outside of the simulation, even outside of our Europe map, which is not a good fit at this stage. There could be many reasons to justify this such as the data or the carbon dating process may have some errors or there might be some cereal pollens at some place before the Neolithic era.

At 3000 BCE

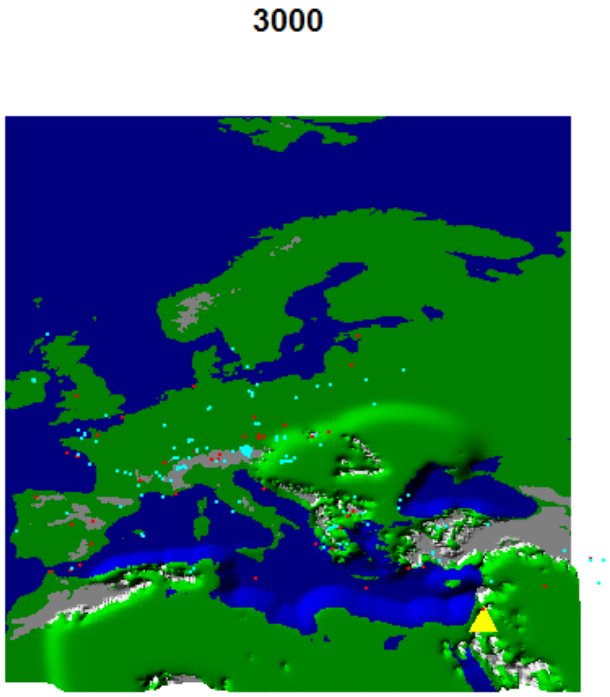

Figure 4.9 Simulation of the Neolithic Population in Europe and Near East at 3000BCE.

The Figure 4.5 show the simulation of the Neolithic population with no advection at 3000BCE. The starting point is Jericho, which is represented by yellow triangle in the plot. The sites of cereal pollen are shown by dots. Red dots represents the pollen sites from 10000BCE up to 3000BCE whereas the cyan dots shows the location of cereal pollen at that particular age bracket i.e. from 4000BCE to 3000BCE.

It is clear from the Figure 4.5 that still there are not many site locations that matches the simulation. Only 56 site locations out of 525 site locations of cereal pollen are matched whereas simulation is showing 88 possible site locations. There are many site locations that are outside of the simulation, even outside of our Europe map, which is not a good fit at this stage. There are probably same reasons to justify this such as the data or the carbon dating process may have some errors or there might be some cereal pollens at some place before the Neolithic era.

At 2000 BCE

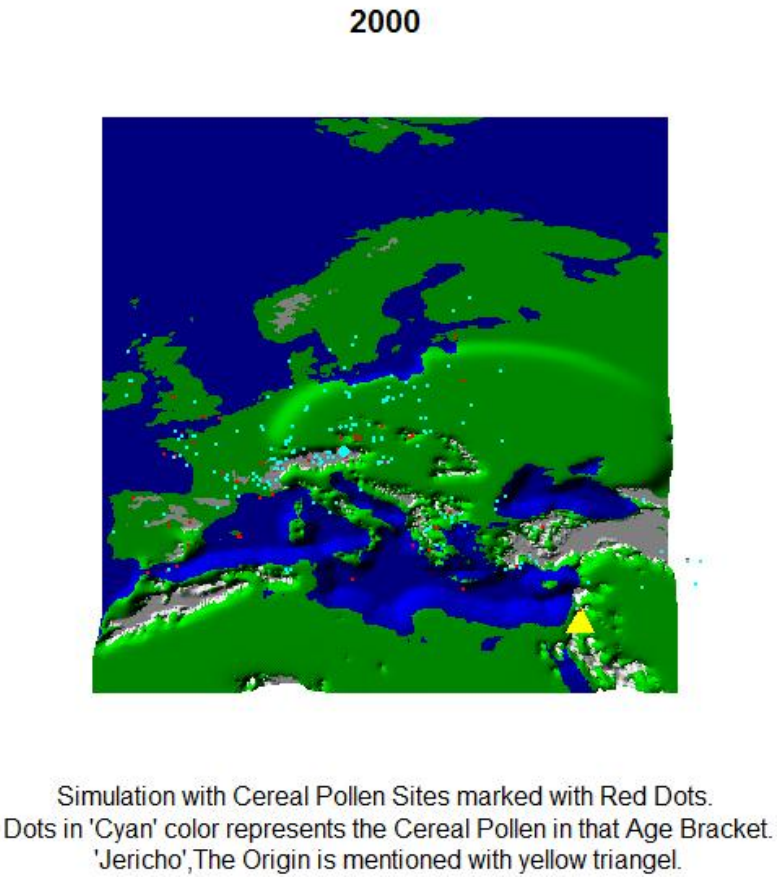

Figure 4.10 Simulation of the Neolithic Population in Europe and Near East at 2000BCE.

The Figure 4.6 show the simulation of the Neolithic population with no advection at 2000BCE. The starting point is Jericho, which is represented by yellow triangle in the plot. The sites of cereal pollen are shown by dots. Red dots represents the pollen sites from 10000BCE up to 2000BCE whereas the cyan dots shows the location of cereal pollen at that particular age bracket i.e. from 3000BCE to 2000BCE.

It is clear from the Figure 4.6 that there are not as many site locations that matches the simulation. 173 site locations out of 780 site locations of cereal pollen are matched whereas simulation is showing 292 possible site locations. Still there are many site locations that are outside of the simulation, even outside of our Europe map. It does not look bad in the site matching but the Neolithic are thought to be spread in the Europe at around 3500BCE, so still this fit is not a good fit at this stage. There could be many reasons to justify this such as the data or the carbon dating process may have some errors or there might be some cereal pollens at some place before the Neolithic era.

At 1000 BCE

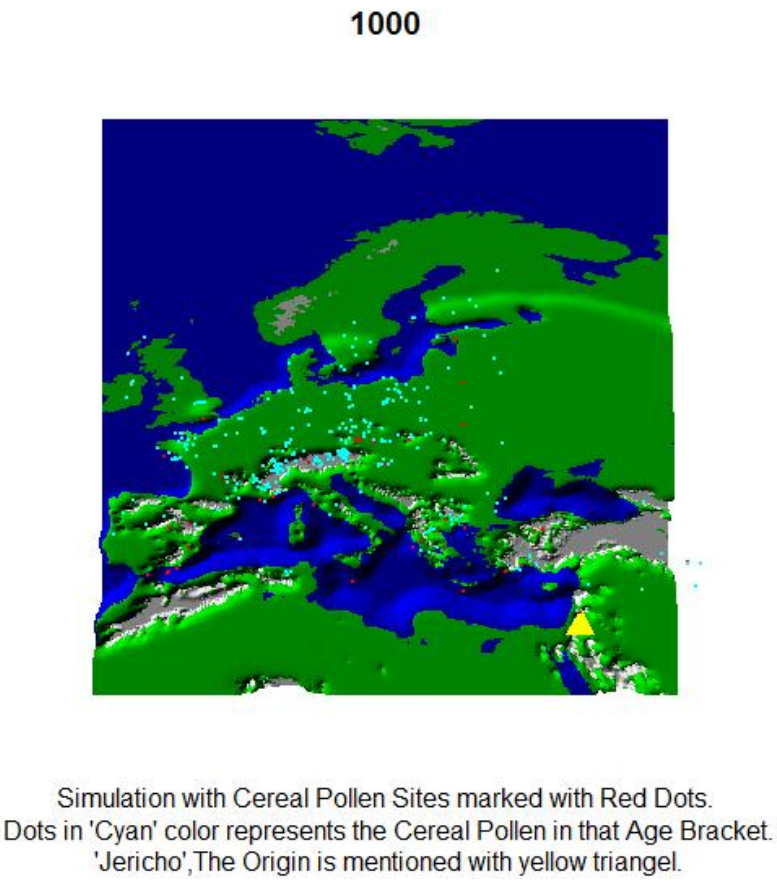

Figure 4.11 Simulation of the Neolithic Population in Europe and Near East at 1000BCE.

The Figure 4.7 show the simulation of the Neolithic population with no advection at 1000BCE. The starting point is Jericho, which is represented by yellow triangle in the plot. The sites of cereal pollen are shown by dots. Red dots represents the pollen sites from 10000BCE up to 1000BCE whereas the cyan dots shows the location of cereal pollen at that particular age bracket i.e. from 2000BCE to 1000BCE.

It is clear from the Figure 4.7 that there are many site locations that matches the simulation. 427 site locations out of 1161 site locations of cereal pollen are matched whereas simulation is showing 618 possible site locations. There are not many site locations that are outside of the simulation. Again, as it is mentioned in the last plot that the fit looks good but it is not good at this point of time. There could be many reasons to justify this such as the data or the carbon dating process may have some errors or there might be some cereal pollens at some place before the Neolithic era. We might have to add advection of moving faster along the water ways to accelerate the movement of the Neolithic population.

At 0 BCE

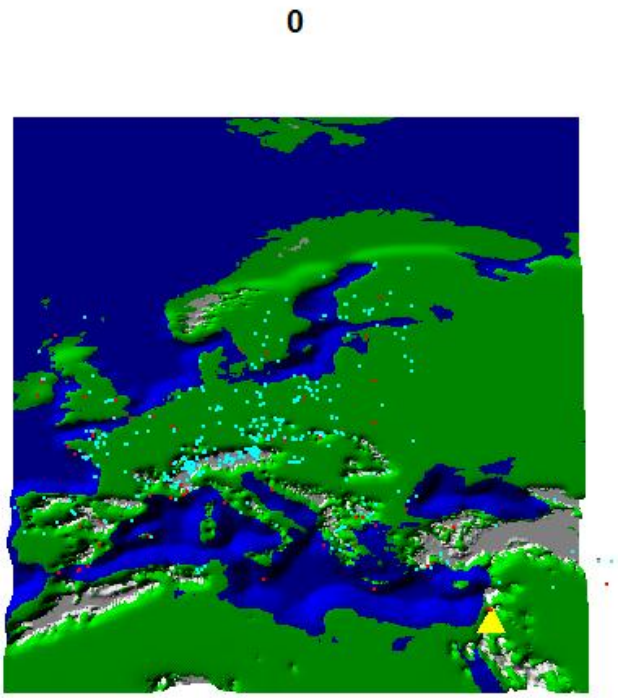

Figure 4.12 Simulation of the Neolithic Population in Europe and Near East at 0BCE.

The Figure 4.8 show the simulation of the Neolithic population with no advection at 0BCE. The starting point is Jericho, which is represented by yellow triangle in the plot. The sites of cereal pollen are shown by dots. Red dots represents the pollen sites from 10000BCE up to 0BCE whereas the cyan dots shows the location of cereal pollen at that particular age bracket i.e. from 1000BCE to 0BCE.

It is clear from the Figure 4.8 that there are many site locations that matches the simulation. 782 site locations out of 1656 site locations of cereal pollen are matched whereas simulation is showing 974 possible site locations. Although, it looks like a good fit but still at this time frame, it cannot be called a good fit. There could be the same reasons to justify this such as the data or the carbon dating process may have some errors or there might be some cereal pollens at some place before the Neolithic era. As it is mentioned in the last plot, the advection probably gives better results.

Full data set at full scale

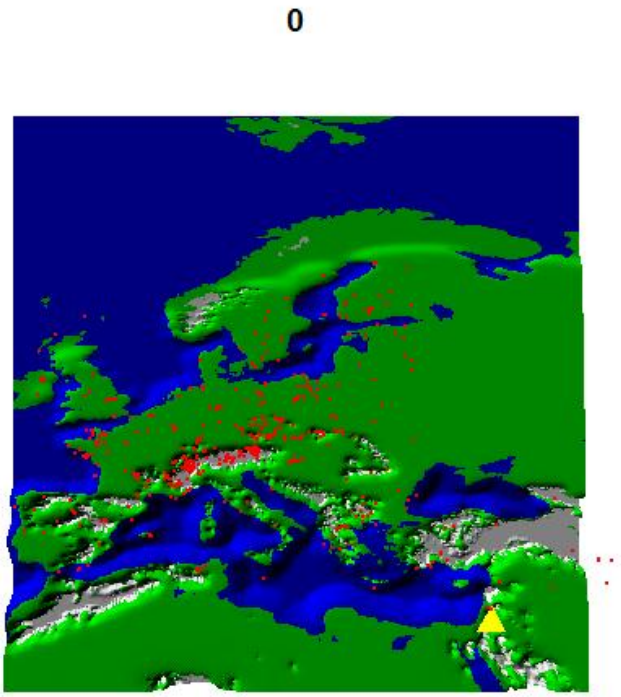

Figure 4.13 Simulation of the Neolithic Population in Europe and Near East from 8000BCE to 0BCE.

The Figure 4.9 show the complete simulation of the Neolithic population with no advection from 8000BCE to 0BCE. The starting point is Jericho, which is represented by yellow triangle in the plot. The sites of cereal pollen are shown by red dots.

It is clear from the Figure 4.9 that there are 782 site locations out of 1656 site locations of cereal pollen are matched whereas simulation is showing 974 possible site locations. There are some site locations that are outside of the simulation, actually outside of our Europe map. So overall it looks like a good fit but the time taken by simulation is not very good. There could be many reasons to justify this such as the data or the carbon dating process may have some errors or there might be some cereal pollens at some place before the Neolithic era. Using advection will also be a good idea which I have used to compare the both results.

4.6 With Advection

Advection refers to preferential movement in particular directions. Here I will use the same model to simulate the Neolithic population but with the addition of advection term “V”, which is a 331×331 matrix. The value of advection velocity will depends on the latitude and longitude. The movements of Neolithic population thought to be slow at high altitudes. Similarly there might have faster movements along Mediterranean coastline and Rhine Danube valleys.

At 7000 BCE

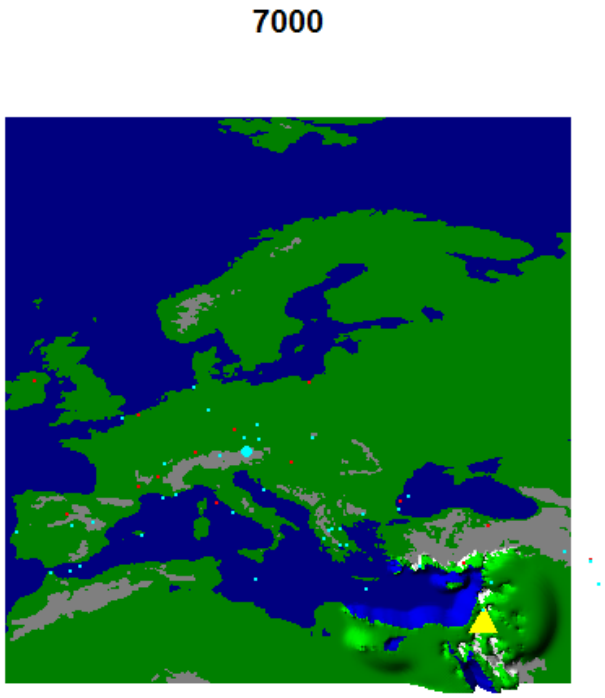

Figure 4.14 Simulation of the Neolithic Population in Europe and Near East at 7000BCE.

The Figure 4.10 show the simulation of the Neolithic population with advection at 7000BCE. The starting point is Jericho, which is represented by yellow triangle in the plot. The sites of cereal pollen are shown by dots. Red dots represents the pollen sites from 10000BCE up to 7000BCE whereas the cyan dots shows the location of cereal pollen at that particular age bracket i.e. from 8000BCE to 7000BCE.

It is clear from the Figure 4.10 that there are not many site locations that matches the simulation. Only 2 site locations out of 53 site locations of cereal pollen are matched whereas simulation is showing 4 possible site locations. There are many site locations that are outside of the simulation, even outside of our Europe map. So this is not a good fit at this stage. There could be many reasons to justify this such as the data or the carbon dating process may have some errors or there might be some cereal pollens at some place before the Neolithic era.

At 6000 BCE

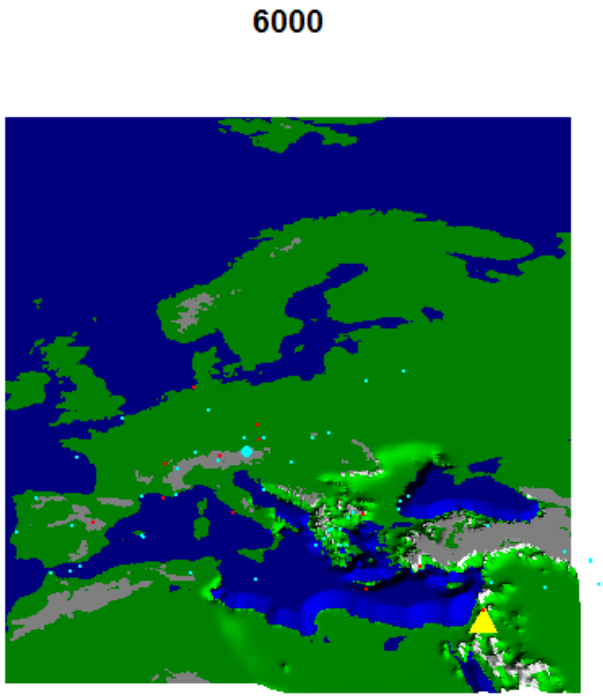

Figure 4.15 Simulation of the Neolithic Population in Europe and Near East at 6000BCE.

The Figure 4.11 show the simulation of the Neolithic population with advection at 6000BCE. The starting point is Jericho, which is represented by yellow triangle in the plot. The sites of cereal pollen are shown by dots. Red dots represents the pollen sites from 10000BCE up to 6000BCE whereas the cyan dots shows the location of cereal pollen at that particular age bracket i.e. from 7000BCE to 6000BCE.

It is clear from the Figure 4.11 that there are not as many site locations that matches the simulation. Only 21 site locations out of 217 site locations of cereal pollen are matched whereas simulation is showing 36 possible site locations. There are many site locations that are outside of the simulation, even outside of our Europe map. Again, it does not looks like a good fit at this stage. There could be many reasons to justify this such as the data or the carbon dating process may have some errors or there might be some cereal pollens at some place before the Neolithic era.

At 5000 BCE

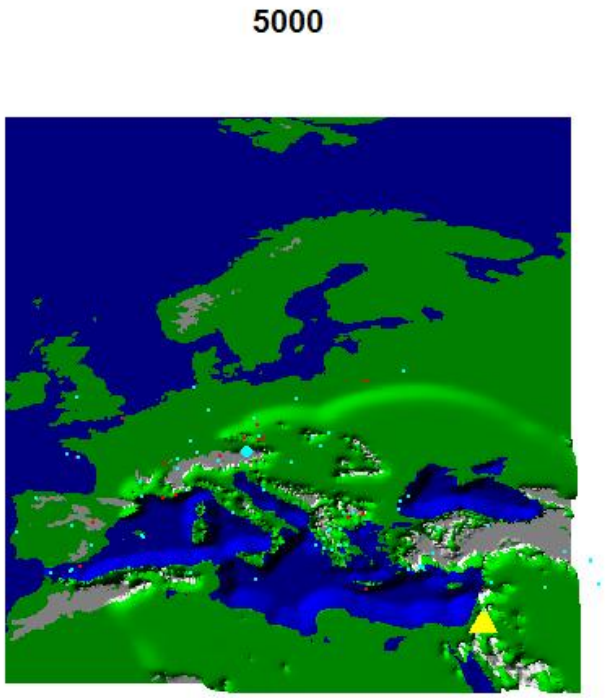

Figure 4.16 Simulation of the Neolithic Population in Europe and Near East at 5000BCE.

The Figure 4.12 show the simulation of the Neolithic population with advection at 5000BCE. The starting point is Jericho, which is represented by yellow triangle in the plot. The sites of cereal pollen are shown by dots. Red dots represents the pollen sites from 10000BCE up to 5000BCE whereas the cyan dots shows the location of cereal pollen at that particular age bracket i.e. from 6000BCE to 5000BCE.

It is clear from the Figure 4.12 that there are not many site locations that matches the simulation. Only 59 site locations out of 217 site locations of cereal pollen are matched whereas simulation is showing 172 possible site locations. There are many site locations that are outside of the simulation, even outside of our Europe map. Still it does not look like a good fit at this stage. There could be many reasons to justify this such as the data or the carbon dating process may have some errors or there might be some cereal pollens at some place before the Neolithic era.

At 4000 BCE

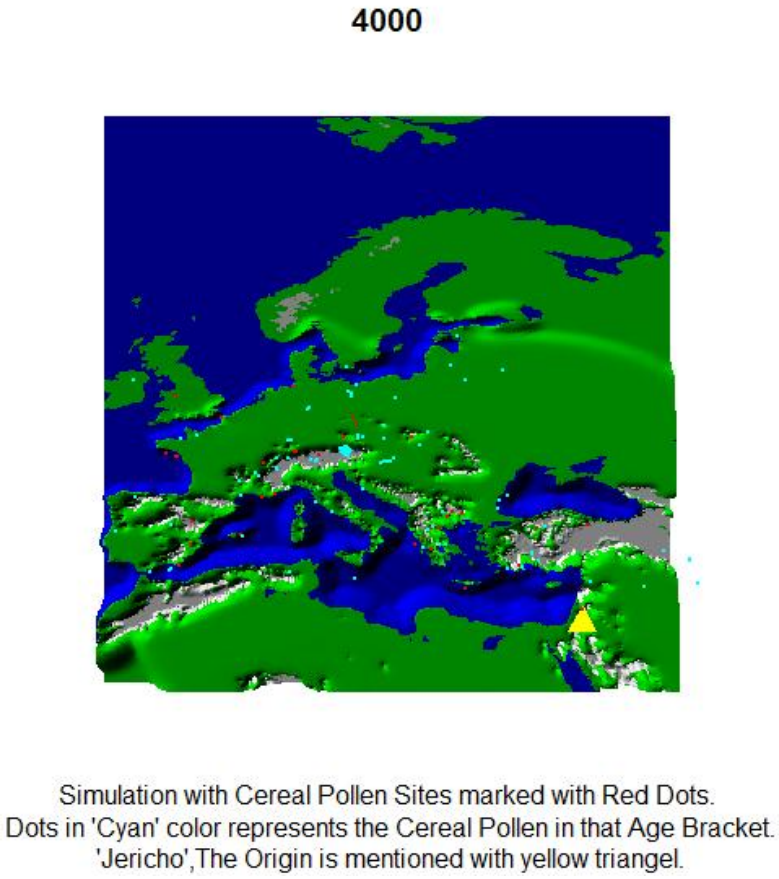

Figure 4.17 Simulation of the Neolithic Population in Europe and Near East at 4000BCE.

The Figure 4.13 show the simulation of the Neolithic population with advection at 4000BCE. The starting point is Jericho, which is represented by yellow triangle in the plot. The sites of cereal pollen are shown by dots. Red dots represents the pollen sites from 10000BCE up to 4000BCE whereas the cyan dots shows the location of cereal pollen at that particular age bracket i.e. from 5000BCE to 4000BCE.

It is clear from the Figure 4.13 that there are many site locations that matches the simulation. 152 site locations out of 346 site locations of cereal pollen are matched whereas simulation is showing 500 possible site locations. The result of this simulation is also matching with the results by Davison et al (2006), which say that the Neolithic population spread into Europe at around 3500BCE. Still there are some site locations that are even outside of our Europe map. But it looks like a good fit with some reservations on the quality and carbon dating process of the data.

At 3000 BCE

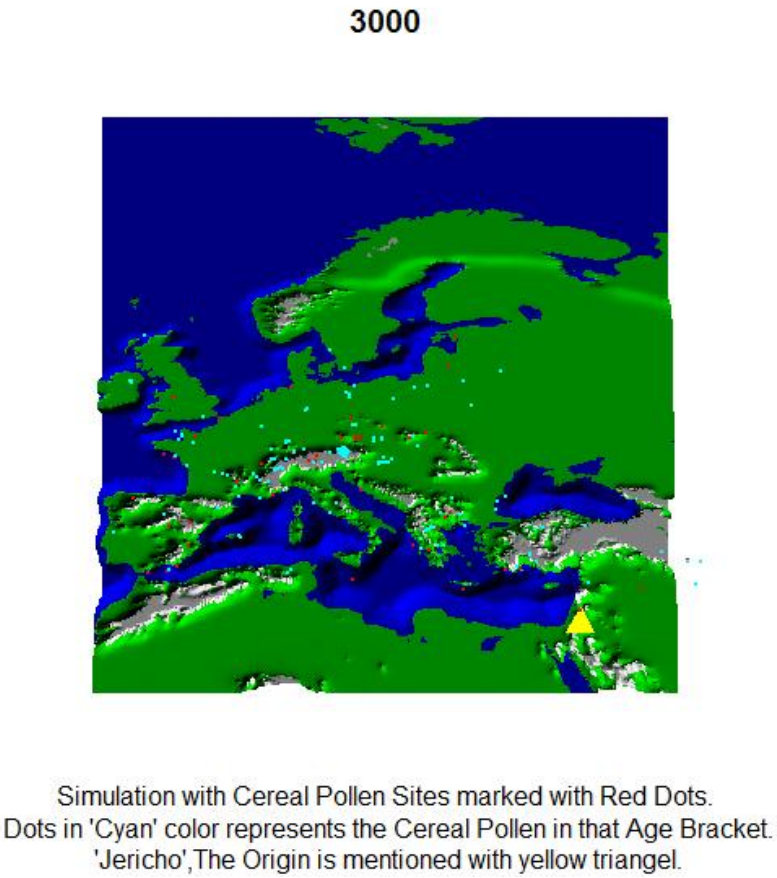

Figure 4.18 Simulation of the Neolithic Population in Europe and Near East at 3000BCE.

The Figure 4.14 show the simulation of the Neolithic population with advection at 3000BCE. The starting point is Jericho, which is represented by yellow triangle in the plot. The sites of cereal pollen are shown by dots. Red dots represents the pollen sites from 10000BCE up to 3000BCE whereas the cyan dots shows the location of cereal pollen at that particular age bracket i.e. from 4000BCE to 3000BCE.

It is clear from the Figure 4.14 that there are many site locations that matches the simulation. 289 site locations out of 525 site locations of cereal pollen are matched whereas simulation is showing 866 site locations. There are some site locations that are outside of the simulation, even outside of our Europe map. But it seems like a good fit with the same possible reservations as mentioned in the last plot.

At 2000 BCE

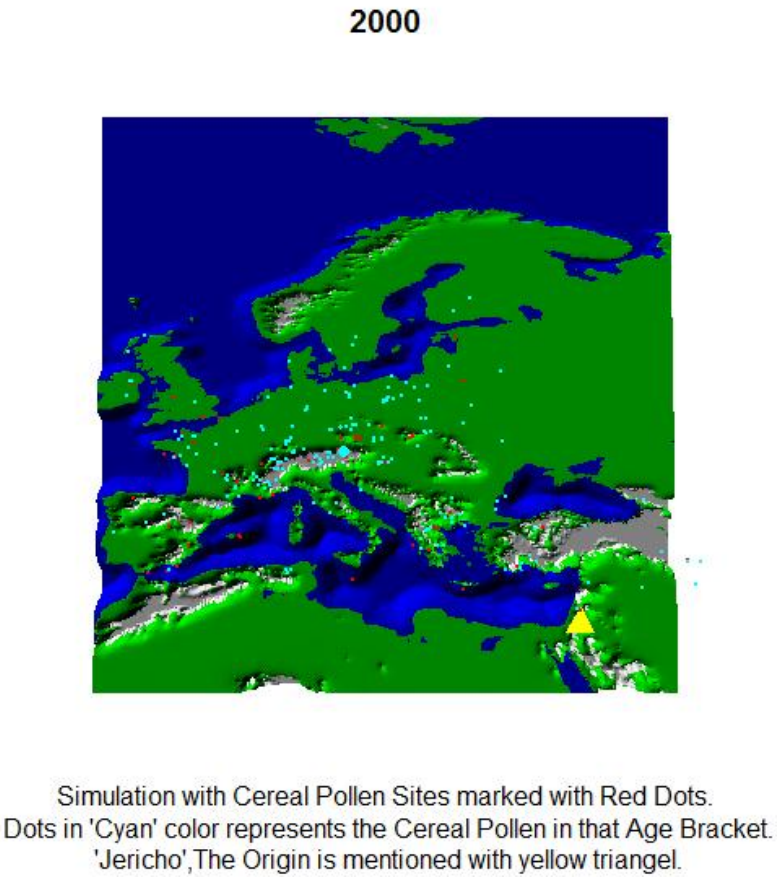

Figure 4.19 Simulation of the Neolithic Population in Europe and Near East at 2000BCE.

The Figure 4.15 show the simulation of the Neolithic population with advection at 2000BCE. The starting point is Jericho, which is represented by yellow triangle in the plot. The sites of cereal pollen are shown by dots. Red dots represents the pollen sites from 10000BCE up to 2000BCE whereas the cyan dots shows the location of cereal pollen at that particular age bracket i.e. from 3000BCE to 2000BCE.

It is clear from the Figure 4.15 that there are many site locations that matches the simulation. 481 site locations out of 780 site locations of cereal pollen are matched whereas simulation is showing 1232 site locations. Still there are some site locations that are outside of the simulation, probably they are outside of our Europe map. It might be a good idea in future to extend the Europe map towards East to accommodate those site locations. Overall it looks like a good fit at this stage.

Full data on full time scale

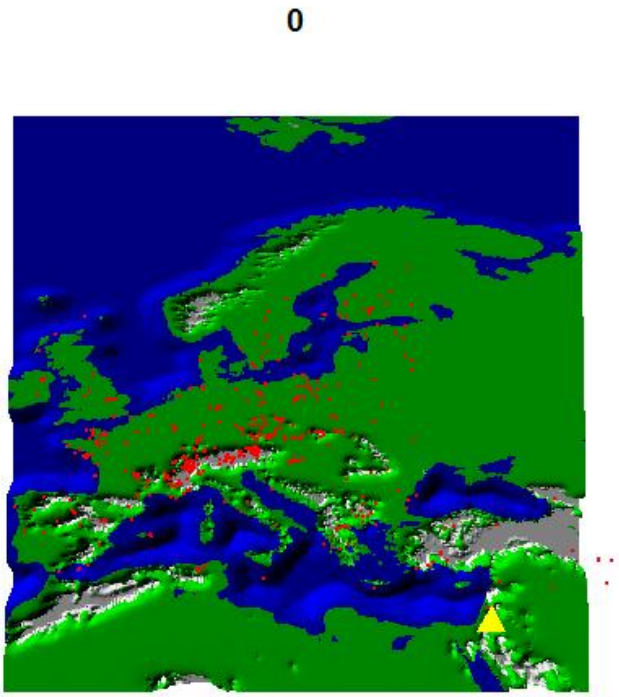

Simulation with Cereal Pollen Sites marked with Red Dots.
Dots in 'Cyan' color represents the Cereal Pollen in that Age Bracket.
'Jericho',The Origin is mentioned with yellow triangel.

Figure 4.20 Simulation of the Neolithic Population in Europe and Near East from 8000BCE to 0BCE.

The Figure 4.16 show the complete simulation of the Neolithic population with advection from 8000BCE to 0BCE. The starting point is Jericho, which is represented by yellow triangle in the plot. The sites of cereal pollen are shown by red dots.

It is clear from the Figure 4.16 that there are 1132 site locations out of 1656 site locations of cereal pollen are matched whereas simulation is showing 1965 possible site locations. There are some site locations that are outside of the simulation, actually outside of our Europe map. So overall it looks like a good fit.

As it is clear from the comparison of the above two simulation models, that the model with advection fits better than that of with no advection. The aim of this work is to formulate and develop a model for the spread of incipient farming in Europe, taking account of such influences of environmental factors. The particular environmental factors considered are the altitude, latitude, opportunity of sea travel, major rivers and coastlines. Although, in this study the only Rhine and Danube rivers were included.

Chapter 5

Possible Improvements and Plan for the Future

According to Cruciani et al. (2004), the agricultural expansion is now often viewed as a leap-frog migration, with comparatively small groups establishing semi-permanent settlements in agricultural oases along major rivers or sea coasts, and partially budding off further afield, when the population reaches a critical mass. The model presented here imagines a continues flow of dispersal.

Fort and Mendez (1999) describe a diffusion model that incorporates interactions between an expanding Neolithic populations with a pre-existing Mesolithic population. Implementing such as interaction in this study would improve the realism of the demographic model.

A further degree of realism could be added to the model by applying advection favoring movement from higher to lower altitudes, so that populations preferentially expanded along lowland plains.

There are several sources of uncertainty inherent in radio-carbon dating, so the dating of the sediment layers found in slices of the cores can be provided in the form of probability distributions. Estimates of arrival times could then include an aspect of this uncertainty.

The diffusion model is the most well developed so far, but there is little new in the current model beyond what has been described in the paper in which it was introduced. For future project, the key goal will be to determine which parameters most affect the reported arrival times. This will give an indication of the uncertainty in the diffusion model with respect to the parameter choices. If only a small set of parameters have a substantial effect on the arrival times, these parameters can be concentrated on during inference.

There is the possibility that more than one advance was made into Europe at the same time, potentially from different directions. The diffusion of more than one population is trivial if no interaction is assumed between the populations. However, there are diffusion models developed that explicitly model interaction between different diffusing entities.

The next important phase of the project will be developing a model to determine the arrival time of cereal to a region. This will require the separation of the signal and noise from the sediment core data. Cereal incidence at sites that are relatively

geographically close, and hence should be near replicates of the cereal arrival process, could give an indication of the strength of noise and temporal uncertainty we might expect in the core samples.

The subsequent goal will be to link the two processes – that is, the human dispersal process, which is entirely predictive, and the process of cereal movement, as revealed by the cores. The most likely approach will be to use estimates of the cereal arrival times, incorporating all uncertainty from radiocarbon dating, noise, dating inference etc., to inform the parameter choices for the diffusion process to try and get dates of arrival for humans and cereal to be as close as possible (or perhaps with a consistent lag, reflecting the time for the cereal crops to flourish).

REFERENCES

National Geophysical Data Center.

The National Geophysical Data Center (NGDC), located in Boulder, Colorado, is a part of the US Department of Commerce (USDOC), National Oceanic & Atmospheric Administration (NOAA), National Environmental Satellite, Data and Information Service (NESDIS).

http://www.ngdc.noaa.gov/mgg/coast/

European Pollen Database.

The European Pollen Database (EPD) is a freely available database of pollen frequencies, past and present, in the larger European area. The database is hosted by the "Institut Méditerranéen d'Ecologie et de Paléoécologie".

http://www.europeanpollendatabase.net/data/

Ammerman, A.J., and Cavalli-Sforza, L.L., (1971). Measuring the rate of spread of early farming in Europe. Man, **6**, PP 674–688.

Ammerman A.J., Cavalli-Sforza L.L. (1973). A population model for the diffusion of early farming in Europe. In*: Renfrew C, editor. The explanation of culture change.* London: Duckworth. pp. 343–357.

Ammerman A.J, Cavalli-Sforza L.L. (1984). The Neolithic Transition and the Genetics of Populations in Europe. *Princeton University Press*, *Princeton.*

Ammerman A.J., Biagi P. (Eds.), (2003). The Widening Harvest. The Neolithic Transition in Europe: Looking Back, Looking Forward. *Archaeological Institute of America*, Boston, MA.

Anderson D.G. (1990). The Paleoindian colonization of Eastern North America: a view from the southeast United States, in Early Paleoindian economies of eastern North America, in: K.B. Tankersley, B.L. Isaac (Eds.), *Research in Economic Anthropology,* Supplement 5. 163-216.

Bar-Yosef O., Belfer-Cohen A. (1992). From foraging to farming, in: Gebauer A.B., Douglas Price T.D. (Eds.), *Transitions to Agriculture in Prehistory,Monographs in World Archaeology* 4. 21-48.

Chernykh E.N., Orlovskaya L.B. (2004). Radiouglerodnaya hrohologiya eneoliticheskih kul'tur yugo-vostochnoi Evropy (Radiocarbon chronology of Neolithic cultures of South-Eastern Europe), Rossiiskaya Arheologiya 4. 24-37.

Childe V.G. (1925). *The Dawn of European Civilization*. Kegan, Paul, Trench and Trubner, London.

Davison K., Dolukhanov P. M., Sarson G. R., Shukurov A (2006). The role of waterways in the spread of Neolithic. *Journal of Archaeological Science 33* (641-652).

Clark J.G.D., (1965). Radiocarbon dating and the expansion of farming culture from the Near East over Europe. *Proceedings of the Prehistoric Society* 31. 57-73.

Cruciani F., La Fratta R., Santolamazza P., Sellitto D., Pascone R., Moral P., Watson E., Guida V., Beraud Colomb E., Zaharova B., Lavinha J., Vona G., Aman R., Calı F., Akar N., Richards M., Torroni A., Novelletto A., Scozzari R., (2004). Phylogeographic analysis of haplogroup E3b (E-M215) Y chromosomes reveals multiple migratory events within and out of Africa. *The American Journal of Human Genetics* 74. 1014-1022.

Currat M., Excoffier L. (2005). The Effect of the Neolithic expansion on European molecular diversity. *Proceedings of the Royal Society B*. 272, No.1564. 679-688

Czaran T. (1997). Spatiotemporal Models of Population Dynamics, Chapman and Hall.

Davison k., Dolukhanov P.M., Sarson G.R., Shukurov A., Zaitseva G.I. (2009). Multiple Sources of the European Neolithic: Mathematical modelling constrained by radiocarbon dates. *Quaternary International 203* (1-2).

Dolukhanov P.M. (1979). *Ecology and Economy in Neolithic Eastern Europe*, Duckworth, London.

Dolukhanov P., Shukurov A., Gronenborn D., Sokoloff D., Timofeev V., Zaitseva G., (2005).The chronology of Neolithic dispersal in Central and Eastern Europe, *Journal of Archaeological Science* 32 1441-1458.

Edmonson M. (1961). Neolithic diffusion rates, *Current Anthropology* 2, 71-102.

Fick A, Poggendorff's Annalen. (1855) 94, 59-86. And (in English) Phil.Mag. S.4, Vol.10, 30-39.

Fisher R.A. (1937). *The wave of advance of advantageous genes, Annals of Eugenics* 7, 355-369.

Fort J, Méndez V (1999). Time-delayed theory of the Neolithic transition in Europe. *Physical Review Letters* Vol 82 Issue4: 867–870.

Fort J., Mendez V., (1999). Reaction-diffusion waves of advance in the transition to agricultural economies. *Physical Review E* 60. 5894-5901.

Gkiasta M., Russell T., Shennan S., Steele J. (2003). Neolithic transition in Europe: the radiocarbon record revisited, *Antiquity* 77 45-61.

Gronenborn D., (2003). Migration, acculturation and culture change in western temperate Eurasia 6500-5000 cal. BC, *Documenta Praehistorica* XXX. 79-91.

Harris D.R., (1996). The origins and spread of agriculture and pastoralism in Eurasia: an overview, in: D.R. Harris (Ed.), *The Origins and Spread of Agriculture and Pastoralism in Eurasia*. Smithsonian Institution Press, Washington, DC. 552-574.

Haslett J., Whiley M., Bhattacharya S., Salter-Townshend M., Wilson S.P., Allen J.R.M., Huntley B., and Mitchell F.J.G. (2006), Bayesian palaeoclimate

reconstruction. *Journal of the Royal Statistical Society*: Series A (Statistics in Society), 169: 395-438.

Hundsdorfer W. and Verwer J. (2003). Numerical Solution of Time-Dependent Advection-Diffusion-Reaction Equations. Springer.

Libby W.F. (1955). *Radiocarbon dating* (2nd Ed.). Chicago: University of Chicago Press.

Kolmogorov A.N., Petrovskii I.G., Piskunov N.S. (1937). A study of the diffusion equation with increase in the quantity of matter, and its application to a biological problem. *Bulletin of Moscow University, Mathematics Series* A 1, 1-25.

Murray J.D. (1993). *Mathematical Biology*, second ed. Springer-Verlag, Berlin.

Okubo A., (1980). Diffusion and Ecological Problems: Mathematical Models, *Springer-Verlag.*

Ozdogan M. (1997). The beginning of Neolithic economies in South-eastern Europe. *Journal of European Archaeology* 5 (2). 1-33.

Perles C. (2001).The Early Neolithic in Greece. The First Farming Communities in Europe. *Cambridge University Press*, Cambridge.

Price T.D. (2000). *Europe's first farmers: an introduction*. Cambridge University Press, Cambridge.1-18

Price T.D., Bentley R.A., Luning J., Gronenborn D., Wahl J., (2001).Prehistoric human migration in the Linearbandkeramik of Central Europe, Antiquity 75. 593-603.

Richards M.B., Corte-Real H., Forster P., Macaulay V., Wilkinson-Herbots H., Demaine A., Papiha S., Hedges R., Bandelt H.–J., Sykes B.C., (1996). Palaeolithic and Neolithic lineages in the European mitochondrial gene pool. *American Journal of Human Genetics* 59. 185-203.

Roussault-Laroque J., (1990). Rubane´ et Cardial, le poids de l'ouest, Rubane´ et Cardial, 39, ERAUL, Lie`ge, 315-360.

Steele J., Adams J., Sluckin T. (1998). Modelling Paleoindian dispersals. *World Archaeology* 30 286-305.

Taylor, R.E. (1987). Radiocarbon Dating*: An Archaeological Perspective*. Academic Press, Orlando.

Troy C.S., Macglugh D.E., Bailey J.F., Magee D.A., Laftus R.G., Cunnigham P., Sykes B.C., Bradley D.G., (2001). Genetic evidence for Near Eastern progons of European cattle, *Nature* 410 1088-1091.

Ucko P.J., Dimbleby G.W. (1969). The Domestication and Exploitation of Plants and Animals. *Duckworth*, London.

Vavilov N. I. (1926), Centry proiskhozhdeniya kul'turnyh rastenii (The centres of origin of cultivated plants). *Bulletin of Applied Botany*, XVI No. 2

Whittle A. (1996). Europe in the Neolithic. The Creation of New Worlds. Cambridge University Press, Cambridge.

Zilhao J. (2001). Radiocarbon evidence for maritime pioneer colonization at the origins of farming in west Mediterranean Europe. *Proceedings of the National Academy of Sciences of the United States of America* 98. 14180-14185.

Zvelebil, M. (1996). The agricultural frontier and the transition to farming in the circum-Baltic region. *In "The Origins and Spread of Agriculture and Pastoralism in Eurasia." (D. R.Harris, Ed.),* pp. 323-345. UCL Press, London.

Appendix A

The following species labels were taken as to be cereal pollens for the purpose of this project.

cf.Triticum, Cerealia-type (excl. Secale), Cerealia-ype/Triticum/Avena, Elymus, cf. Triticum diccocon, Cerealia undifferentiated, Cerealia/Secale, Cerealia (excl. Secale), Cereales, Cerealia indeterminate, cf. Avena, Poaceae undifferentiated >40µm, Cerealia-type, cf. Secale, Poaceae large, Elymus-type, cf. Hordeum, Hordeum/Secale, Cerealia-type/Secale, Cerealia sp., Gramineae >43µm, Secale-type, Glyceria maxima, Cerealia.

Appendix B

R Codes for Diffusion Function

These R codes are provided by Dr. Steven Miller and been reproduce here with his permission.

Simple.Diffuse.Func

```
simple.diffuse.func<-
function (my.grid, nsim = 10000, K = K.mat,
v = v.mat, gamma = gamma.mat,
coastline = coastline.mat + rhine.danube.mat,
V = V.mat, freq = 100,
particular.points = NULL)
{   advection.time = 0
nr = nrow(my.grid)
nc = ncol(my.grid)
i = dist.func(1, 1, 1, 2)/6
g = sapply(lat.vec, function(x) {dist.func(1, x, 2,
x)})/6
```

```
r = 6356.7523
coastline[coastline > 1] = 1
coastline.right.mat <- cbind(coastline[, -1],
coastline[,nc])
coastline.left.mat <- cbind(coastline[, 1], coastline[, -
nc])
coastline.above.mat <- rbind(coastline[1, ], coastline[-
nr,])
coastline.below.mat <- rbind(coastline[-1, ],
coastline[nr,])
v.above1.grid = rbind(v.mat[1, ], v.mat[-nr, ])
v.below1.grid = rbind(v.mat[-1, ], v.mat[nr, ])
v.left1.grid = cbind(v.mat[, 1], v.mat[, -nc])
v.right1.grid = cbind(v.mat[, -1], v.mat[, nc])
Rlat <- 1/r * (coastline.right.mat -
coastline.left.mat)/(2 * i)
Rlong <- t(1/(r * sin(lat.vec)) * t(coastline.below.mat -
coastline.above.mat)/(2 * g))
Rnorm <- sqrt(Rlat^2 + Rlong^2)
Vhatlong <- (-Rlat)/Rnorm
Vhatlat <- Rlong/Rnorm
Vhatlong[Rnorm == 0] = 0
Vhatlat[Rnorm == 0] = 0
time = 0
```

```
my.grid.list = list(my.grid)
names(my.grid.list)[1] = time
new.grid = my.grid
last.rec.time = time
if (!is.null(particular.points))
{grid.long.index <- sapply(particular.points$Long,
function(x)
{which.min((x - long.vec)^2)})
grid.lat.index <- sapply(particular.points$Lat,
function(x) {
which.min((x - lat.vec)^2)})
particular.result <- data.frame(entity =
particular.points$entity,
GridLat = lat.vec[grid.lat.index], GridLong =
long.vec[grid.long.index])
particular.result <- cbind(particular.result, `0` =
sapply(1:nrow(particular.points),
function(x) {my.grid[grid.long.index[x],
grid.lat.index[x]]}))}
start.time = proc.time()[3]
while (time < nsim)
{old.grid = new.grid
above1.grid = rbind(old.grid[1, ], old.grid[-nr, ])
below1.grid = rbind(old.grid[-1, ], old.grid[nr, ])
```

```
left1.grid = cbind(old.grid[, 1], old.grid[, -nc])
right1.grid = cbind(old.grid[, -1], old.grid[, nc])
delNx <- t(t(below1.grid - above1.grid)/(2 * g))
deldelNx <- t(t(below1.grid - 2 * old.grid +
above1.grid)/(g^2))
delNy <- (right1.grid - left1.grid)/(2 * i)
deldelNy <- (right1.grid - 2 * old.grid +
left1.grid)/(i^2)
delvx <- t(t(v.below1.grid - v.above1.grid)/(2 * g))
delvy <- (v.right1.grid - v.left1.grid)/(2 * i)
new.grid.row = delvx * delNx + v.mat * deldelNx
new.grid.col = delvy * delNy + v.mat * deldelNy
diffusion = new.grid.row + new.grid.col
normDelN <- sqrt(delNx^2 + delNy^2)
Shatx <- (-delNx)/normDelN
Shaty <- (-delNy)/normDelN
Shatx[normDelN == 0] = 0
Shaty[normDelN == 0] = 0
Vmultiplier = V * sign(Shatx * Vhatlong + Shaty *
Vhatlat)
Vx = Vmultiplier * Vhatlong
Vy = Vmultiplier * Vhatlat
advection = Vx * delNx + Vy * delNy
growth = matrix(0, nrow = nr, ncol = nc)
```

```
growth[K > 0] = gamma[K > 0] * old.grid[K > 0] * (1 -
old.grid[K > 0]/K[K > 0])
addition = growth + diffusion - advection
condition = K - old.grid
ratio = condition/addition
A = 1
condition1 <- freq - (time - last.rec.time)
condition2 <- A/(2 * t(v)) * (i^2 * g^2)/(i^2 + g^2)
condition3 <- A/(2 * t(abs(Vx))) * g
condition4 <- A/(2 * abs(Vy)) * i
h = min(ifelse(condition1 > 0, condition1, Inf),
condition2[condition2 > 0])
time = time + h
new.grid = old.grid + h * addition
if (any(new.grid[alt.mat >= 0] > K)) {
warning(paste(sum(new.grid[alt.mat >= 0] > K),
"cells with density exceeding capacity at time", time))
new.grid[new.grid > K & alt.mat >= 0] = K[new.grid >
K & alt.mat >= 0]}
if (any(new.grid < 0)) {
warning(paste(sum(new.grid < 0),
"cells with negative density at time", time))
new.grid[new.grid < 0] = 0 }
if (any(new.grid > max(K))) {
```

```
new.grid[new.grid > max(K)] = max(K) }
if ((time - last.rec.time) >= freq | time >= nsim) {
if (!is.null(particular.points)) {
particular.result <- cbind(particular.result,
sapply(1:nrow(particular.points), function(x) {
new.grid[grid.long.index[x], grid.lat.index[x]]}))
names(particular.result)[ncol(particular.result)] = time}
else { my.grid.list[[length(my.grid.list) + 1]] =
new.grid
names(my.grid.list)[length(my.grid.list)] = time }
current.time = proc.time()[3]
duration = current.time - start.time
remaining = duration * (nsim/time - 1)
print(paste("Elapsed: ", round(duration/60, 1), " min
To go: ",
round(remaining/60, 1), " min", sep = ""))
flush.console()
last.rec.time = time}}
if (!is.null(particular.points))
return(particular.result)
else return(my.grid.list)}
```

```
temp = diffuse.plot(result.list)
temp= diffuse.plot(result.list,7)
pollen<- read.csv(file.choose(),header=TRUE)

points(trans3d(35.44054,31.83764,5,temp),pch=17,cex=2,col
="yellow")

points(trans3d(pollen[,3],pollen[,2],5,temp),pch=16,cex=p
ollen[,11]/max(pollen[,11],na.rm=TRUE),col="red")

diffuse.plot(result.list,5)

pollen.now=apply(as.matrix(pollen[,9:12]),1,sum,na.rm=TRU
E)
points(trans3d(pollen[,3],pollen[,2],5,temp),pch=16,cex=p
ollen.now/max(pollen.now),col="red")

pollen.now=apply(as.matrix(pollen[,9]),1,sum,na.rm=TRUE)
points(trans3d(pollen[,3],pollen[,2],5,temp),pch=16,cex=p
ollen.now/max(pollen.now),col="cyan")

# note the first column is from Jericho (e.g. 8000 years
ago, say)
particular.df=pollen[-c(498:503),1:3]
```

```
colnames(particular.df)=c("entity","Lat","Long")
diffuse.df=simple.diffuse.func(my.grid,particular.points=
particular.df)
diffuse2.df= round(diffuse.df[-c(1:3)])

diffuse2.df[diffuse2.df>0]=1  ### CONVERT ROUNDED
DENSITIES TO 0 OR 1

pollen21=pollen2[-c(1:3)]
pollen22=pollen21[-c(10:11)]
pollen7=pollen22[-(498:503),]



## to check the fit for the observed and simulated data
##at Age Brackets
##result is mismatch
result=abs(diffuse2.df[,2:5]-pollen7[,9:6])
sum(result)
sum(diffuse2.df[,2:5])
sum(pollen7[,9:6])
match= (sum(pollen7[,9:6])+sum(diffuse2.df[,2:5])-
sum(result))/2
match
```

R Code for Diffusion Plot

```
diffuse.plot <-
function (grid.list, frames, phi = 90, theta = 0, ...)
{  if (missing(frames))
frames = 1:length(grid.list)
nr <- nrow(grid.list[[1]])
nc <- ncol(grid.list[[1]])
ave.alt.mat <- (alt.mat[-nr, -nc] +
alt.mat[-1, -nc] +
alt.mat[-nr,-1] + alt.mat[-1, -1])/4
col.mat <- matrix("green", nrow = nr - 1,
ncol = nc - 1)
col.mat[ave.alt.mat >= 1000] = "white"
col.mat[ave.alt.mat < 0] = "blue"
for (i in frames)
persp(long.vec, lat.vec, grid.list[[i]],
scale = FALSE, box = FALSE, border = NA,
shade = 1, phi = phi,
theta = theta, main = names(grid.list)[i],
col = col.mat, ...)}
```

```
result.list=simple.diffuse.func(my.grid)


diffuse.plot(result.list)
```

Appendix C

This is the list of sediment core sites from the European Pollen Database (EPD), where cereal pollen was detected.

Site Name	Latitude	Longitude
Abant Gölü	40.6	31.28333
Aegelsee	46.64583	7.543333
Ageröds Mosse	55.83333	13.41667
Aghia Galini	35.1	24.68333
Ahlenmoor	53.7	8.733333
Ahlequellmoor	51.73056	9.509444
Aholami	61.88333	25.21667
Akgöl Adabag	37.5	33.73333
Älbi Flue	46.35556	7.583611
Aletschwald	46.23222	8.014167
Algendar	39.94056	3.958611
Almenara de Adaja	41.19194	-4.66806
Alp Lüsga Belalp 1	46.23083	7.590278
Alpi di Robièi Val Bavona	46.44389	8.516944
Alsópáhok	46.77444	17.17028

Altenweiher	48.01333	6.994444
Ampoix	45.63333	2.933333
Amsoldingersee	46.725	7.575
Amtkel	43.26806	41.30833
Anenské údolí	50.58861	16.1175
Anse de Gattemare	49.69278	-1.29806
Anse Saint-Martin	49.70389	-1.87861
Antas	37.20833	-1.82361
Arkutino Lake	42.36667	27.73333
Aronde	49.4625	2.691111
Arts Lough	52.95	-6.43333
Auneau	48.45611	1.793611
Avrig	45.71667	24.38333
Bajondillo	36.61972	-4.49639
Baldeggersee	47.16667	8.283333
Barbora	48.94167	14.93333
Basse-Ville	47.18611	-1.85806
Beaufort Birkenbach	49.84722	6.125833
Beliya Kanton	41.73361	24.13972
Bellefontaine	46.57528	6.093056
Berdorf Aesbaach	49.81944	6.371111
Beysehir Gölü I	37.54167	31.5
Bibersee	47.13056	8.28

Biot	43.8	7.1
Biskupinskie Lake	52.78333	17.73333
Bitsch-Naters	46.20278	7.592778
Bjärsjöholmssjön	55.45	13.78333
Blainville-sur-Orne	49.20306	-0.30889
Blato	49.04167	15.19167
Bledowo Lake	52.55	20.66667
Bobrov	49.44583	19.56667
Bodmen Alp Bel	46.21444	7.575
Boehnigsee Goldmoos	46.25917	7.843056
Bokanjacko	44.18333	15.23333
Borkovicka blata	49.21667	14.9
Bouara	35.23333	41.18333
Bourdim	36.80333	8.253889
Branna	48.95	14.93333
Brede Bridge	50.92861	0.599722
Breidfeld	50.12278	6.063056
Breitnau-Neuhof	47.93333	8.066667
Brentenlohe	49.78722	12.4625
Bruchberg	51.75889	10.46
Bruckmisse	48.7325	8.644167
Buntes Moor	47.0625	11.30333
Burmarrad ria	35.935	14.41444

Butter Mountain	54.16667	-6.03333
Cala Galdana	39.93694	3.965
Cala'n Porter	39.87056	4.131389
Canaleja	40.9	-2.45
Carrivmoragh	54.31667	-5.98333
Cergowa Gora	49.53333	21.7
Cerná Hora	50.66056	15.75583
Cervene blato	48.85	14.93333
Change-Glatinier	48.11667	-0.78889
Charco da Candieira	40.34167	-7.57639
Chef-du-Pont	49.38194	-1.36056
Chrást	50.22722	14.54417
Colfiorito	43.025	12.925
Correo	44.50833	5.983056
Coulvain	49.06667	-0.71667
Csögle	47.21583	17.255
Czajkow	50.78333	21.28333
Dags Mosse	58.33333	14.7
Dar Fatma	36.81667	8.766667
Darzlubie Forest	54.7	18.16667
Delta del Rio Besos	41.38028	2.248333
Djebel El Ghorra	36.5975	8.394722
Dolgoe	55.23333	28.18333

Dortmunder Hütte	47.1	11
Dovjok Swamp	48.75	28.25
Dry Lake II	42.05	23.53333
Dunum (Hilliges Moor)	53.58333	7.633333
Dura-Moor	46.64	11.45889
Durchenbergried	47.78333	8.983333
Dürrenecksee-Moor	47.16667	13.86667
Dury	53.63889	18.35833
Dvur Ansov	48.79167	16.3875
Edessa	40.81806	21.9525
Egelsee	47.6125	12.17083
Eggen ob Blatten	46.22167	7.5925
Embouchac	43.56639	3.916667
Ennerie	47.24028	-2
Etang de Cheylade	45.09	2.895
Etang de la Gruère	47.23972	7.049167
Etang de Luissel Bex	46.14139	7.010278
Etang d'y Cor Montana	46.31056	7.478333
Etang paysan	49.69611	-1.86722
Fangeas	44.71611	6.449444
Färshesjön	56.16667	15.86667
Felchosee	53.05	14.13333
Feuenried	47.75	8.916667

Flaje Kiefern	50.7	13.53333
Fletnowo	53.53333	18.65
Flögeln	53.66667	8.763889
Fontaine Henry	49.2775	-0.45333
Fougères	48.51667	-0.83333
Foula	60.15	-2.1
Fuchsschwanzmoos	47.11667	13.9
Füramoos	47.98333	9.883333
Fuschlsee	47.78333	13.26667
Gaienhofen	47.67944	8.975833
Gamperfin	47.10139	9.225
Garaat El-Ouez	36.81833	8.333333
Georgenfelder Hochmoor	50.75	13.75
Gerlos	47.24306	12.13889
Gerzensee	46.495	7.324722
Ghab	35.68333	36.3
Giannitsa B	40.66667	22.31667
Giecz	52.31944	17.36333
Giering	47.47139	12.35833
Glaswaldsee	48.42667	8.249167
Gleboczek Lake	52.64917	17.63306
Godziszewskie Lake	54.09333	18.55278
Gölhisar Gölü	37.13333	29.6

Gondo Alpjen	46.12417	8.064722
Gorno	50.85	20.83333
Grächen See	46.115	7.504444
Gradenmoos	47.96528	12.80833
Grand Ratz le Pellet	45.34167	5.608333
Greicheralp Riederalp	46.22472	8.014722
Großer Krebssee	52.85	14.1
Grosser Treppelsee	52.15	14.45278
Grosses Überling Schattseit-Moor	47.16667	13.9
Hagelseeli	46.4025	8.021111
Halos I	39.16667	22.83333
Hängstli	46.47361	7.495833
Herrenwiesser see	48.66917	8.296389
Hières sur Amby	45.79083	5.283333
Hinterburgseeli	46.43056	8.040556
Hipper Sick	53.21667	-1.58333
Hockham Mere	52.5	0.833333
Holtjärnen	60.65	14.91667
Holzmaar	50.11667	8.878889
Hopschensee	46.15111	8.012222
Horní Lomná	49.52056	18.63083
Hornstaad/Bodensee	47.7	9.016667

Hort Timoner	39.875	4.126389
Hoya del Castillo	41.25	-0.5
Hoyran Gölü	38.275	30.875
Hrabanoská cernava	50.21639	14.83167
Huleh	33.10556	35.52833
Hurecká Bog	49.15222	13.3275
Huzenbacher See	48.57444	8.348056
Ioannina I	39.7625	20.73056
Ioannina II	39.69194	20.83972
Isokärret	60.21667	22.13333
Jasiel	49.37278	21.88694
Jelení louze	50.89278	14.27
Jezioro Druzno	54.11667	19.46667
Kaarkotinlampi	61.41667	25.86667
Kaartlamminsuo	60.73333	24.21667
Kalsa Mire	58.16667	27.45
Kamenicky	49.73333	15.96667
Kancelársky prikop	50.64667	16.10417
Kansjon	57.63333	14.53333
Kararmik Batakligi	38.425	30.8
Kassjön	63.91667	20.01667
Kastoria	40.55194	21.32222
Katzenloch	47.34167	11.125

Khimaditis Ib	40.61667	21.58333
Khimaditis III	40.6125	21.58611
King's Pool	52.80833	-2.10833
Kirkkosaari	60.86667	24.5
Kittilä	65.025	24.68333
Kleinen Mochowsee	51.99639	14.19889
Klotjärnen	61.81667	16.53333
Kluki	54.70694	17.28472
Knízecí pláne	48.96472	13.63528
Komoranské jezero	50.5	13.5
Köycegiz Gölü	36.875	28.64167
Kozli	49.37639	14.02583
Krageholmssjön	55.5	13.73333
Královec	49.13194	18.02778
Kraví Hora	50.58417	16.1525
Kuivajarvi	60.78333	23.83333
Kulzer Moos	49.39472	12.44278
Kupena	41.98333	24.33333
La Beuffarde	46.82361	6.423056
La Caudelais	47.26111	-1.78056
La Grande Basse	48.05	6.95
La Molina mire	43.38111	6.327222
La Taphanel	45.27444	2.679167

Labsk∞ dul	50.76611	15.55472
Lac de Bretaye	46.19361	7.042222
Lac de Lod	45.8025	7.609722
Lac de Praver	45.07361	5.856389
Lac de Villa	45.68472	7.761111
Lac des Boites	45.05611	5.885278
Lac du Bouchet	44.91667	3.783333
Lac du Lauzon	44.67528	5.793333
Lac du Mont d'Orge Sion	46.14028	7.202778
Lac Long Inférieur	44.05778	7.45
Lac Miroir	44.63528	6.793889
Lac Noir	45.45361	2.627222
Lac Saint Léger	44.42	6.336389
Lackan Bog	54.26667	-6.08333
Ladik Gölü	40.91667	36.01667
Lago dell'Accesa	42.98639	10.88333
Lago di Bévera	45.51083	8.533889
Lago di Ganna	45.535	8.493889
Lago di Martignano	42.11667	12.33333
Lago Grande di Avigliana	45.065	7.386667
Lago Grande di Monticchio	40.94444	15.6
Lago Piccolo di Avigliana	45.05	7.383333
Lagoa Comprida 2	40.36278	-7.63611

Laguna de la Roya	42.21667	-6.76667
Laguna Guallar	41.4	-0.21667
Laguna Salada Chiprana	41.23333	-0.16667
Lailias	41.26778	23.59944
Lake Almalou	37.66528	46.63194
Lake Balaton (Northeast)	47.00167	18.10417
Lake Balaton (Southwest)	46.81833	17.735
Lake Duranunlak	43.66667	28.55
Lake Ermistu	58.36667	23.96667
Lake Flarken	58.58333	13.66667
Lake Gosciaz	52.58333	19.35
Lake Kolmilaträsk	60.28333	20.15
Lake Kvarnträsk	60.35	19.98333
Lake Lednica	52.55694	17.39028
Lake Mikolajki	53.76806	21.41806
Lake of Annecy	45.85667	6.172222
Lake Orestiás	40.51167	21.25778
Lake Racou	42.55417	2.008333
Lake Racze	53.91667	14.66667
Lake Sambösjön	57.13333	12.41667
Lake Shabla-Ezeretz	43.58333	28.55
Lake Skrzetuszewskie	52.55	17.36056
Lake Solso	56.13333	8.633333

Lake Trummen	56.86667	14.83333
Lake Urmia	37.58333	45.46667
Lake Urmia II	37.79361	45.37583
Lake Van	38.5	43
Lake Varna (Arsenala)	43.2	27.83333
Lake Varna (Beloslav-Poveljanovo)	43.2	27.83333
Lake Voulkaria	38.86667	20.83333
Lake Xinias	39.05	22.26667
Lake Zeribar	35.53333	46.11667
Langes Fenn Kemnitzerheide	52.31361	12.91361
Las Pardillas Lake	42.04556	-3.04528
Lavau	47.30778	-1.96528
Le Fourneau	48.44444	-0.19167
Le Grand Lemps	45.47333	5.416667
Le Jolan	45.13944	2.859167
Le Loclat	47.02028	6.997778
Le Marais de la Perge (South)	45.3825	-1.115
Le Marais St Boetien	49.61667	3.816667
Liivjarve Bog	59.21667	27.58333
Lilla Gloppsjön	59.80444	14.62778
Linden	46.51028	7.410833
Lindenmoos	47.50972	0

Lingreville	48.92972	-1.54306
Liptovsky Jan	49.04167	19.67778
Lobsigensee	47.03194	7.299167
Loch Cleat	57.06667	-6.33333
Lochan an Druim	58.46667	-4.7
Locmariaquer	47.55444	-2.93222
Löddigsee	53.43333	11.85
Logne	47.32833	-1.50111
Long Lough	54.41667	-5.86667
Loras	45.66389	5.244444
Loucky	49.325	15.50278
Lough Henney	54.43333	-5.9
Lüderholz	51.68472	10.30583
Lutinière	46.44444	-0.86222
Lüttersee	51.57667	10.16167
Mabo Moss	58.01667	16.06667
Machová	48.83083	17.54111
Maharlou Lake	29.47722	52.75972
Majen El Orbi	37.15	9.083333
Malá niva	48.91389	13.81611
Maleshevska Mountains Peat Bog	41.7	23.03333
Malhaire	48.5	-1

Malschötscher Hotter	46.66611	11.45833
Maly Suszek	53.72556	17.77278
Marais de Charauze	45.36833	5.566944
Marais de la Perge	45.3975	-1.01028
Marais de Marchesieux	49.17333	-1.3
Mayralampi	62.33333	26.23333
Mekelermeer	52.76667	6.616667
Menez-Cam	48.25	-3.5
Mieminger See	47.29167	10.97639
Mire Garvan	44.11694	26.95
Mire Johvika	58.5	22.33333
Mittlere Hellelen	46.16583	7.503889
Mobeche Forest	48.51667	-1
Moerzeke	51.04833	4.176389
Mohos	46.08333	25.91667
Mokre louky (South)	48.83333	14.83333
Mont Carré Hérémence	46.09139	7.220556
Monte Areo mire	43.52889	-5.76889
Monte San Giorgio	45.90889	8.953889
Montfarville	49.645	-1.25417
Moor Alpenrose	47.08667	11.77861
Moor am Rofenberg	46.82917	10.82556
Moor im Weissenstadter	50.13667	11.88028

Forst		
Moselotte	48.03194	7
Mosfell	64.12611	-20.6097
Mossen	60.11667	21.6
Moulin de Prugnolas	45.84972	1.645833
Mrtv∞ luh	48.86694	13.88306
Mutorog Peat Bog	43.51667	23.61667
Na bahne	50.19889	15.96139
Nad Dolsk∞m ml∞nem	50.8525	14.33889
Nagy-Mohos	48.32694	20.43639
Navarrés	39.1	-0.68333
Novienky peat bog	52.24	54.75111
Nussbaumer Seen	47.61667	8.833333
Oberderdingen-Großvillars	49.0425	8.760278
Olbramovice	48.99167	16.4
Oppligen	46.495	7.353889
Ortasee	45.81667	8.4
Osvea	56.05	28.08333
Palasiny	49.68889	15.48333
Pamerkiai Outcrop	54.31389	24.73611
Pancavská louka	50.76639	15.54111
Pannel Bridge	50.90583	0.675278
Pas du Gu	47.23833	-2.15

Peat-bog Begbunar	42.15	22.55
Pelléautier	44.52222	6.183333
Peschanoe	51.98333	25.48333
Petiville	49.23333	-0.16667
Peyrelevade	45.70833	2.383333
Pierre Folle	47.01889	-1.89306
Pinarbasi	37.46667	30.05
Plaine Alpe	44.96389	6.594167
Plesné jezero	48.77694	13.86583
Pölöske	46.75611	16.92472
Pont-l'Eveque Le Lac	49.275	-0.19972
Popovo Ezero	41.71667	23.66667
Popradské pleso	39.08444	20.07306
Posidonia Lligat	42.29222	-3.29111
Pötréte	46.67889	16.93306
Praz Rodet	46.56528	6.171944
PRD-4	42.53333	-8.51667
Pré Rond	44.91889	6.594167
Pryskyricn∞ dul	50.88778	14.41333
Puerto de Los Tornos	43.15	-3.43333
Puscizna Rekowianska	49.48333	19.81667
Puy de Pailleret	45.51667	2.816667
Quintanar de la Sierra	42.03333	-3.01667

Raigastvere Lake	58.6	26.66667
Ran Viken	56.28333	14.3
Rappershausen	50.37917	10.39139
Rasna	49.23056	15.37083
Redmere	52.43972	0.438056
Refugio Mondovi	44.18333	7.733333
Regetovka	49.425	21.27917
Rezabinec	49.25	14.11667
Riffelsee	45.9825	7.761111
Rinderplatz	46.64472	11.49444
Rodenbourg Bretzboesh	49.69167	6.27
Rokytecká slat	49.01528	13.41194
Roquetas de Mar	36.79444	-2.58889
Rotmoos Obergurgl	46.84167	11.025
Rotmoos-Eriz	46.79417	7.841667
Rotsee	47.07556	8.325556
Rudnickie Male	53.43361	18.75028
Rudushskoe Lake	56.5	27.55
Rybárenská Slat	49.03139	13.46194
Rynholec	50.12944	13.92972
Ryönänsuo	60.43333	24.16667
Sabbion	44.13	7.473333
Sägistalsee	46.67972	7.976389

Saint Hilaire du Rosier	45.14583	5.316667
Saint Julien de Ratz	45.35	5.623333
Saint Sauveur	43.56639	3.916667
Saint Sixte	45.425	5.625
Saint Viaud Contin	47.265	-2.01667
Saint-Thomas	47.26861	-1.75
Saint-Ursin	48.51944	-0.25333
San Rafael	36.77361	-2.60139
Schönwies	46.84861	11.02917
Schöpfenwaldmoor	46.44389	7.505278
Schwarzsee	46.66639	11.43194
Schwarzsee FR	46.67028	7.284722
Schwarzsee Reschenscheideck	46.86972	10.47972
Schwarzsee VS	45.99083	7.705556
Schwemm	47.65	12.3
Seebergsee	46.61667	7.466667
Seefelder See	47.32361	11.19167
Selle di Carnino	44.15	7.694444
Semenic	45.18	22.05944
Serrent	47.80944	-2.46806
Siikasuo	61.3	22.06667
Silberhohl	51.91	10.1825

Simplon/Gampisch-Alter		
Spittel	46.23028	8.011389
Sipola	65.05	24.79167
Slawsko	52.66667	18.25
Slieve Croob	54.33333	-5.98333
Slieve Naslat	54.35	-5.98333
Slopiec	50.78333	20.78333
Sögüt Gölü	36.9975	29.89833
Sommersüss	46.76083	11.67833
Son Bou	39.92472	4.027222
Sonnenberger Moor	51.76806	10.51611
Sredna Gora Mountains Peat		
Bog	42.83333	24.83333
Stará Boleslav	50.19806	14.6675
Steerenmoos	47.8	8.2
Steklin	52.93333	18.98333
Stoyanov 2	50.38333	24.63333
Strázenská slat	48.89889	13.74222
Strazym Lake	53.33333	19.46111
Strbské pleso	49.12222	20.05556
Suchedniow	51.05	20.85
Süftenenegg	46.73333	7.398056
Svarcenberk	49.14583	14.705

Svatoborice-Mistrin	48.83333	17.16667
Swietokrzyskie Lake	52.54444	17.59861
Syrjälänsuo	61.21667	28.11667
Szigliget	46.8	17.43333
Szymbark	49.63333	21.1
Tarnawa Wyzna	49.1	22.83333
Tarnowiec	49.7	21.61667
Tauernmoos	47.17222	12.64444
Tenaghi Philippon	40.98333	24.78333
Teplické údolí	50.585	16.13167
Thorpe Bulmer	54.71667	-1.3
Tisice	50.23694	14.53278
Tlstá hora	48.89417	17.88861
Tocqueboeuf	49.68889	-1.41667
Tondi	59.46667	24.91667
Tourbière de Gatimort	43.57528	2.785556
Tourbière de la Lande	43.56667	2.966667
Tourbière de la Peyroutarié	44.46667	3.6
Tourbière de Mont Sec	45.06889	5.806667
Tourbière de Pilaz	45.81694	7.833333
Tourbière de Raux	44.50333	5.935278
Tourbière de Santa Anna	45.85833	7.654167
Tourbière des Narses Mortes	44.43333	3.6

Tourbière des Nassettes	44.46667	3.641667
Tourbière du Peschio	44.45	3.6
Tourves	43.5	5.9
Trikhonis 5	38.6	21.5
Troarn Saint-Samson	49.18361	-0.16806
Trogenmoos	46.76056	7.8625
Trumer Moos	47.93333	13.06667
Tullerinsuo	61.33333	21.95
Turbera de La Panera Cabras	40.16583	-5.75806
Tyre	33.27806	35.20306
Tytuvenu Tyrelis	55.58333	23.3
Uitbergen	51.01778	3.944722
Umbrail	46.54278	10.42083
Unter-Ückersee	53.25	13.85
Vallée de la Voise	48.41667	1.75
Vasikkasuo	64.66667	27.86667
Vauville	49.63611	-1.84889
Vegoritis 8	40.75	21.75
Velká niva	48.92417	13.81861
Velky Ded	50.08333	17.21667
Velky Maj	50.05	17.21667
Vernerovice	50.62167	16.19583
Vinderhoute	51.07917	3.622778

Vitosha Mountains Peat Bog	42.83333	23.83333
Vladar	50.08	13.21778
Vlci rokle	50.60444	16.12833
Vracov	48.97778	17.20278
Wachel 3	53.43889	8.868889
Wachseldorn Untermoos	46.82056	7.733889
Wallbach Lenk	46.42722	7.401944
Wangen/Bodensee	47.66667	8.933333
Waschhorn	53.615	8.736944
Wasenmoos	47.30583	12.4175
Wasenmoos beim Zellhof	47.98333	13.1
Watten	50.83361	2.213333
Waxeckalm	47.02	11.5
Weiherlohe	49.72972	12.3875
Welney Washes	52.51667	0.25
Wilder See beim Ruhestein	48.56972	8.236944
Wildmoos	46.95	11.01806
Wildseemoor bei Kaltenbronn	48.71972	8.458889
Willingham Mere	52.33972	-0.05722
Wolin II	53.83333	14.66667
Woryty	53.75	20.2
Yeniçaga Gölü	40.78333	32.03333

Ylimysneva	62.13333	22.86667
Zalavár	46.78528	17.155
Zarnowiec Peat Bog	54.71667	18.11667
Zbudovska blata	49.83333	14.33056
Zirbenwaldmoor	46.85833	11.025
Zlatnicka Dolina	49.51667	19.28333
Θpské raseliniste Mire	50.73889	15.7125